NAVAL POSTGRADUATE SCHOOL
Monterey, California

DTIC
S ELECTE
DEC 0 4 1992
B
D

THESIS

Reference Path Generation and Tracking
of
Marine Vehicles

by

Timothy J. Panoff

September, 1992

Thesis Advisor: Fotis A. Papoulias

Approved for public release; distribution is unlimited

REPORT DOCUMENTATION PAGE

1a. REPORT SECURITY CLASSIFICATION Unclassified	1b. RESTRICTIVE MARKINGS

2a. SECURITY CLASSIFICATION AUTHORITY	3. DISTRIBUTION/AVAILABILITY OF REPORT
2b. DECLASSIFICATION/DOWNGRADING SCHEDULE	Approved for public release; distribution is unlimited.

4. PERFORMING ORGANIZATION REPORT NUMBER(S)	5. MONITORING ORGANIZATION REPORT NUMBER(S)

6a. NAME OF PERFORMING ORGANIZATION Naval Postgraduate School	6b. OFFICE SYMBOL (If applicable) 34	7a. NAME OF MONITORING ORGANIZATION Naval Postgraduate School

6c. ADDRESS (City, State, and ZIP Code) Monterey, CA 93943-5000	7b. ADDRESS (City, State, and ZIP Code) Monterey, CA 93943-5000

8a. NAME OF FUNDING/SPONSORING ORGANIZATION	8b. OFFICE SYMBOL (If applicable)	9. PROCUREMENT INSTRUMENT IDENTIFICATION NUMBER

8c. ADDRESS (City, State, and ZIP Code)

10. SOURCE OF FUNDING NUMBERS

Program Element No.	Project No.	Task No.	Work Unit Accession Number

11. TITLE (Include Security Classification)
REFERENCE PATH GENERATION AND TRACKING OF MARINE VEHICLES

12. PERSONAL AUTHOR(S) Timothy J. Panoff

13a. TYPE OF REPORT Master's Thesis	13b. TIME COVERED From　　To	14. DATE OF REPORT (year, month, day) September, 1992	15. PAGE COUNT 65

16. SUPPLEMENTARY NOTATION
The views expressed in this thesis are those of the author and do not reflect the official policy or position of the Department of Defense or the U.S. Government.

17. COSATI CODES			18. SUBJECT TERMS (continue on reverse if necessary and identify by block number)
FIELD	GROUP	SUBGROUP	Reference Path, Equtions of Motion, LQR

19. ABSTRACT (continue on reverse if necessary and identify by block number)

This thesis analyzes the problem of acurate path keeping for marine vehicles. The reference path is generated automatically through the use of a critically damped second order model. An appropiate shift in the time axis allows a smooth path with zero oveshoot regardless of the initial conditions. Control design for the physical system is achieved through the use of optimum control and linear quadratic regulator techniques. Results are presented for general maneuvering scenarios in the horizontal plane and demonstrate the validity of the models used in the research.

20. DISTRIBUTION/AVAILABILITY OF ABSTRACT ☒ UNCLASSIFIED/UNLIMITED　☐ SAME AS REPORT　☐ DTIC USERS	21. ABSTRACT SECURITY CLASSIFICATION unclassified	
22a. NAME OF RESPONSIBLE INDIVIDUAL Fotis A. Papoulias	22b. TELEPHONE (Include Area code) (408) 646-3381	22c. OFFICE SYMBOL ME/Pa

DD FORM 1473, 84 MAR　　83 APR edition may be used until exhausted　　SECURITY CLASSIFICATION OF THIS PAGE
All other editions are obsolete　　Unclassified

Reference Path Generation and tracking
of
Marine Vehicles

by

Timothy J. Panoff
Lieutenant , United States Navy
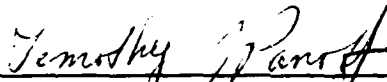B.S., Virginia Military Institue, 1986

Submitted in partial fulfillment
of the requirements for the degree of

MASTER OF SCIENCE IN MECHANICAL ENGINEERING

from the

NAVAL POSTGRADUATE SCHOOL
September, 1992

Author: _____

Timothy J. Panoff

Approved by: _____

Fotis A. Papoulias, Thesis Advisor

_____

Matthew D. Kelleher, Chairman
Department of Mechanical Engineering

ABSTRACT

This thesis analyses the problem of accurate path following for marine vehicles. The reference path is generated automatically through the use of a critically damped second order model. An appropriate shift in the time axis allows a smooth path with zero overshoot regardless of the initial conditions. Control design for the physical system is achieved through the use of optimum control and linear quadratic regulator techniques. Results are presented for general maneuvering scenarios in the horizontal plane and demonstrate the validity of the methods used in the research.

DTIC QUALITY INSPECTED 1

iii

TABLE OF CONTENTS

I. INTRODUCTION

Accurate path keeping of a marine vehicle through prescribed routes in space is one of the most important functions of both manned and unmanned vehicles [Ref. 1]. This can be achieved by a number of ways, two of the most popular ones being line of sight [Ref. 2] and cross track error guidance [Ref. 3]. In general, cross track error schemes are superior provided an accurate representation of vehicle dynamics is available. Cross track error control is very efficient for straight line reference paths. Switching between consecutive straight line segments is inaccurate since no reference path is explicitly accounted for [Ref. 3]. This problem is addressed in this work where we concentrate on two different aspects of the general path keeping problem. The first aspect is the generation of a smooth reference path which joins two consecutive straight line segments.

In ship dynamics problems it is necessary to introduce two different coordinate systems [Ref. 4]. A global coordinate system is used to monitor the absolute location of the marine vehicle with respect to a fixed reference point, while a local (x,y) frame is introduced to express the relative location of the vehicle with respect to the desired steady state path. This coincides with the local x-axis, therefore the local frame is recomputed each time a new straight line segment is

commanded. We then seek a smooth reference path that initiates at the current position of the vehicle and terminates at the desired straight line segment, the x-axis. If we nondemensionalize x by the vehicles length L, time t by L, and the constant vehicle forward speed u, then x and t assume identical numerical values at steady state. Therefore, for small deviations in y, a (t,y) graph can be interpreted as (x,y) as well. This allows us to use an ordinary differential equation to model the reference path in the local coordinate frame.

After a smooth reference path has been generated, we proceed with the control design; we seek a rudder control law which will drive and keep the vehicle on the reference path. This is accomplished by using the Linear Quadratic Regulator design [Ref. 5]. A performance index which penalizes the deviation of the actual path from the reference path is formulated and minimized. Finally, we present a series of numerical simulations which support the techniques used in this work, along with some recommendations for further research.

II. REFERENCE PATH DEVELOPMENT

A. INTRODUCTION

We break the problem of generating a smooth reference path for the vehicle to follow into two parts. In the first part, we examine the lane changing maneuver; i.e., the change from one straight line path to a parallel path. Then we address the more general case of path following where the two straight line paths, initial and final form an arbitrary angle on the plane.

B. LANE CHANGING

Figure 2.1 represents the type of path that we are interested in during a lane changing maneuver. This type of path can be achieved when using a differential equation whose solution is exponential. A first order equation would generate a path that is too steep for the vehicle to follow, while on the other hand, a third or higher order equation would result in oscillatory response with multiple overshoots of the desired steady state path. For the purposes of this thesis it was felt that a second order system would provide a good compromise between fast response and smooth changes. By using the second order differential equation
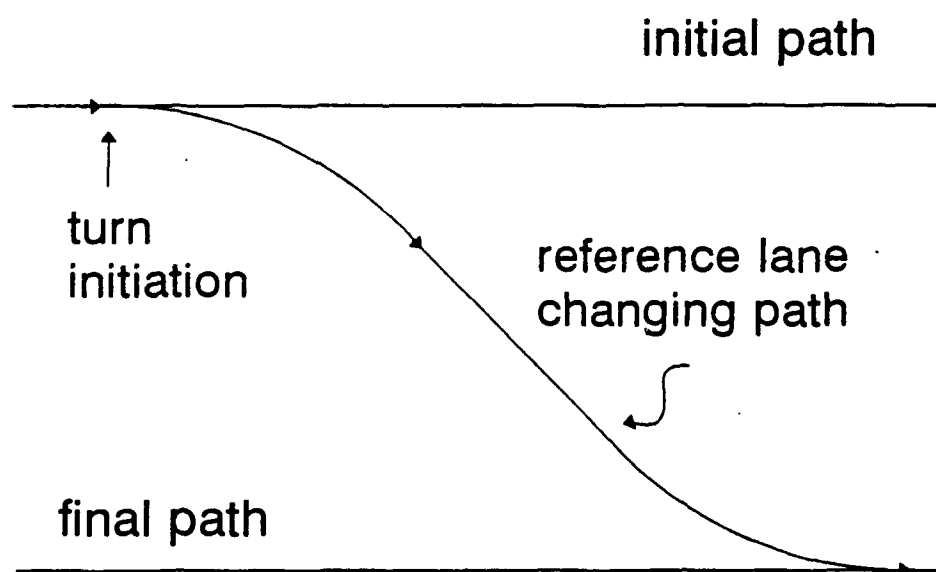
3

Figure 2.1 Desired Reference Path

$$\ddot{y} + 2\zeta\omega_n\dot{y} + \omega_n^2 y = 0 \qquad (2.1)$$

with ζ representing the damping in the system and ω_n representing the speed of the response of the system, the following types of paths can be produced using different ζ and ω_n. (Figures 2.2 and 2.3) The larger the value of ω_n the quicker the system response and the smaller the ζ the more the system over shoots the path.

After review of the above figures, a damping ratio, $\zeta = 1$, was chosen. This seems to provide the smoothest path possible with no overshoot of the path. A natural frequency, $\omega_n = 1$, was chosen to provide a reasonable time response of the system. By choosing $\omega_n = 1$ we have accounted for the fact that a physical system with certain mechanical restraints is being represented and thus we allow for the system to respond as quickly as possible without overworking.

Solving the above differential equation, the following equations are formed:

$$y(t) = y_0 e^{-t}(1+t) \qquad (2.2)$$

$$\dot{y}(t) = -y_0 t e^{-t} \qquad (2.3)$$

Plotting eqn (2.2) the desired reference path shown in figure 2.4 was produced.
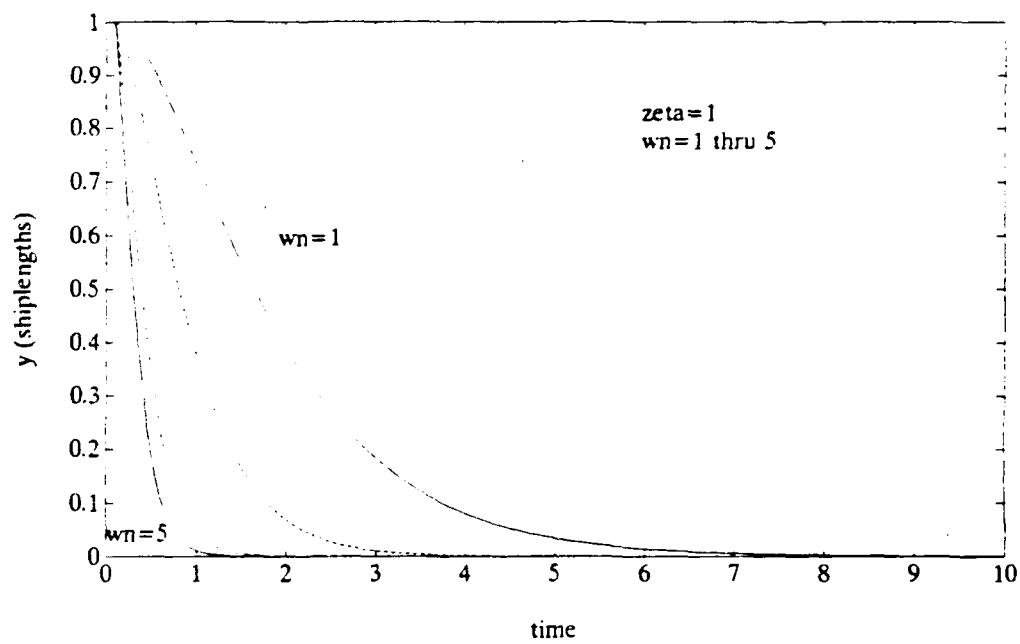
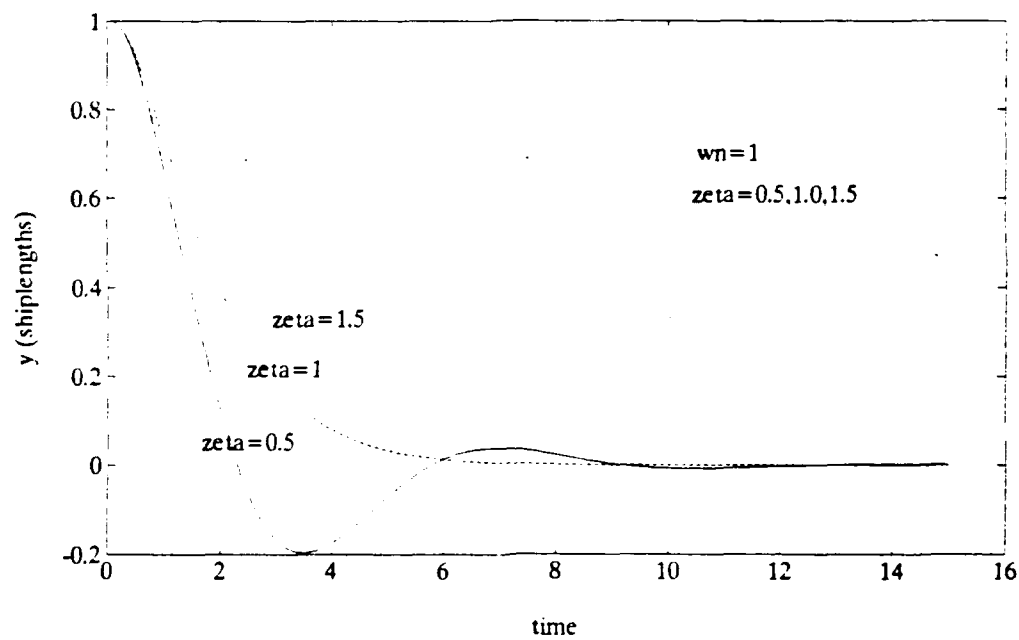Figure 2.2 Different Reference Paths; Fixed ζ and Varying ω_n

Figure 2.3 Different Reference Paths; Fixed ω_n and Varying ζ
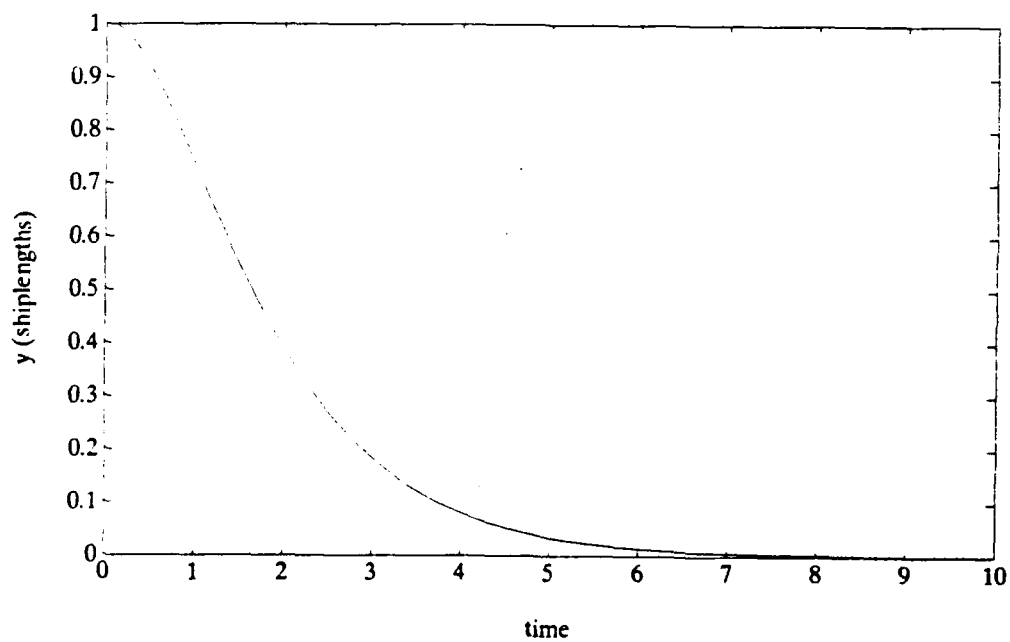
Figure 2.4 Desired Reference Path

C. GENERAL REFERENCE PATHS

In the development of the reference path the angle between the two paths was assumed to be zero. This angle is designated as α. By using different angles between paths, it was found that the smooth path developed for the zero angle was soon lost. As shown in figure 2.5, excessive path overshoot may develop as the angle α approaches 90°. Although the system remains critically damped, the path overshoot is non-zero due to the non-zero initial velocities which is increased as $\alpha \rightarrow 90°$.

It appeared, therefore, that the reference path was only good for a zero angle between the two paths. However, it was felt that if we utilized only that portion of the path that corresponded to the desired angle, a smooth reference path with zero overshoot could still be produced.

This is accomplished by breaking the reference path into two parts. The first is the time that it takes for the path to get to the desired angle α. This is denoted as T shown in figure 2.6. The second is the time to finish the reference path from the angle α. This is denoted as t. The time t is the start point of the portion of the reference path that is needed. In actuality the entire reference path is produced but only that portion of the path that is needed is used in the simulation and control program.

If we assume $dy(0)/dt = v_0$ and $y(0) = a$ we obtain the following from eqns (2.2) and (2.3),

$$v_0 = -y_0 t e^{-t} \qquad (2.4)$$

$$a = y_0 e^{-t} (1+t) \qquad (2.5)$$

with a representing the y axis position and v_0 representing the initial angle from the horizontal of the path which is the same as α. If we divide by v_0 by a we obtain the time it takes to get to angle α.

$$\frac{v_0}{a} \approx -\frac{t}{1+t} \qquad (2.6)$$

This is T. Using T we put this back into our original equation and we get,

$$y(t) = y_0 \exp^{-(t+T)} (1+t+T) \qquad (2.7)$$

$$\dot{y}(t) = -(t+T) y_0 \exp^{-(t+T)}. \qquad (2.8)$$

These equations provide the basis for the desired smooth reference path. A family of reference paths produced using this technique is shown in figure 2.7 for different initial slopes α. It can be seen that incorporating the above time T, the reference path maintains the general shape shown in figure 2.4 regardless of the angle α.

10
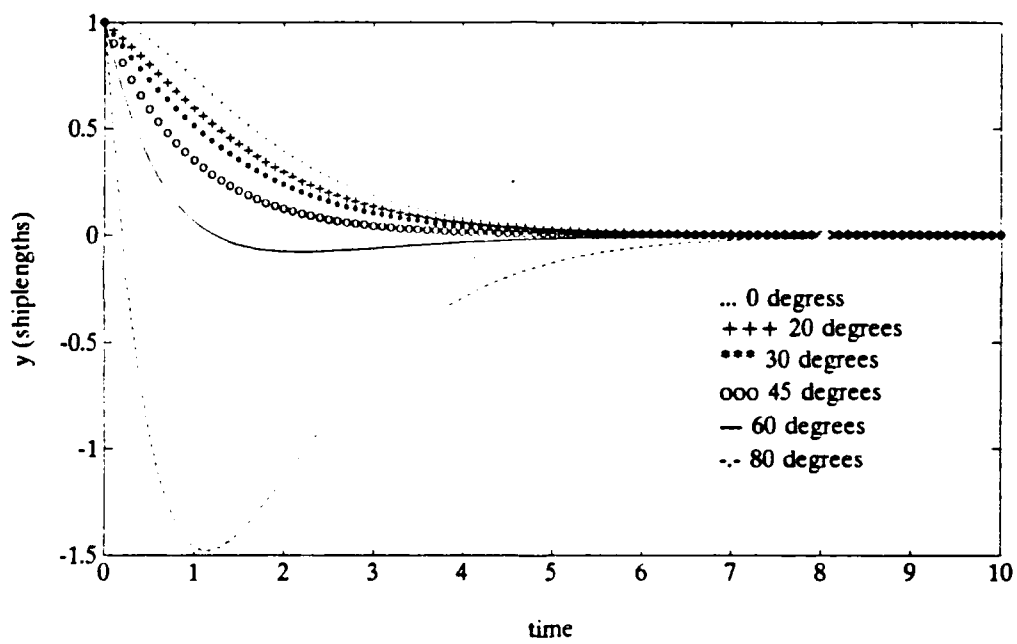
Figure 2.5 Path Overshoot for Varying Angles

11
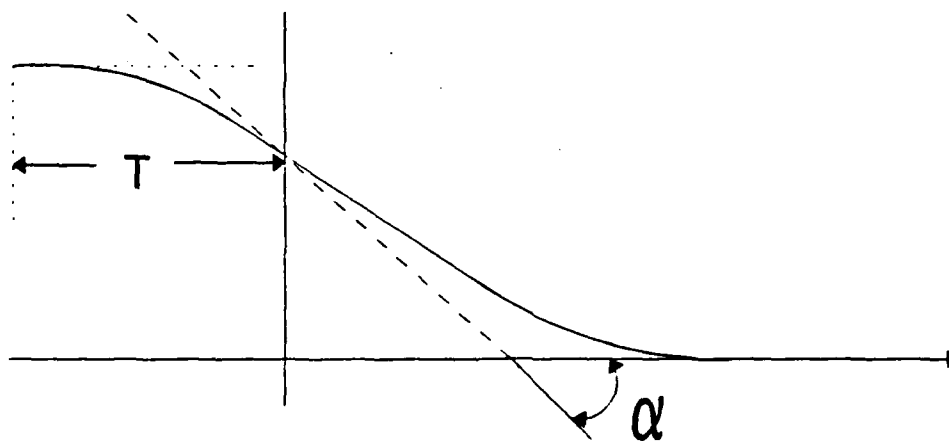
Figure 2.6 Reference Path Configuration
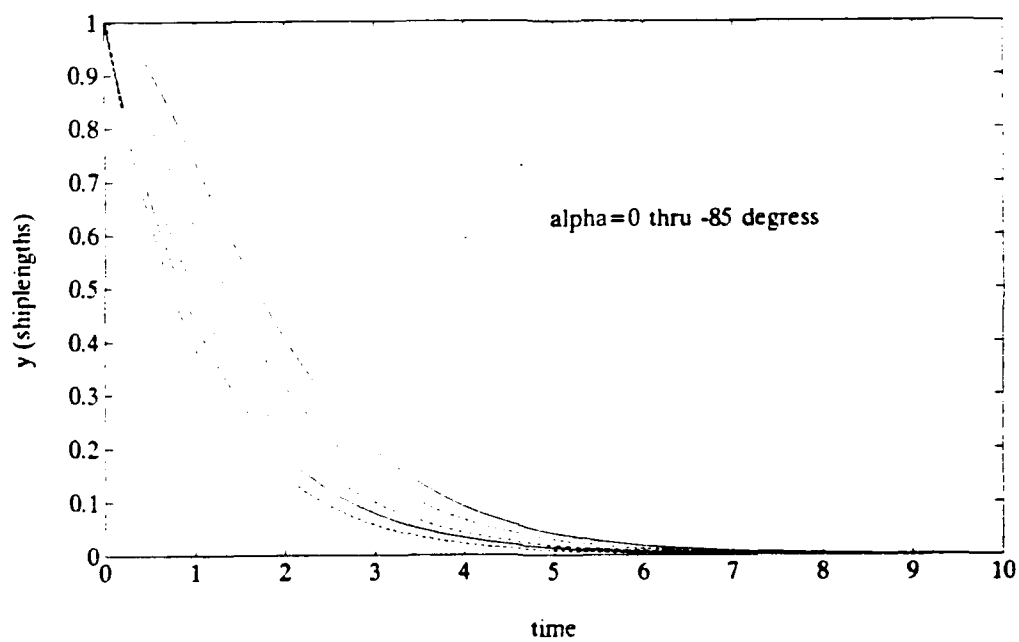
Figure 2.7 Family of Desired Reference Paths

III. EQUATIONS OF MOTION AND LQR MINIMIZATION DEVELOPMENT

A. INTRODUCTION

Now that a reference path has been developed, an overview of the appropriate equations of motion and minimization needs to be presented. We are only concerned with the horizontal plane, which means that only the steering aspect of the test vehicle will be considered. This chapter will examine what are the equations of motions, their augmentation with the reference path equations, and the LQR minimization used in order to obtain controller gains.

B. EQUATIONS OF MOTION

By using a nondimentionalized linearized set of equations of motion for the horizontal plane, the following equations are developed and shown in state space form.

$$\dot{\psi} = r \tag{3.1a}$$

$$\dot{v} = a_{11}v + a_{12}r + b_1\delta \tag{3.1b}$$

$$\dot{r} = a_{21}v + a_{22}r + b_2\delta \tag{3.1c}$$

$$\dot{y} = v\cos(\psi) + \sin(\psi) \tag{3.1d}$$

With $a_{11} = -1.526394$, $a_{12} = -0.5096502$, $a_{21} = 0.028750753$, $a_{22} = -1.449505$, $b_1 = 0.0020674169$, and $b_2 = -2.841506$.

14

The reference path equation (2.1) is written as

$$\dot{y}_{r1} = y_{r2}, \qquad (3.2a)$$

$$\dot{y}_{r_2} = -\omega_n y_{r_1} - 2\zeta\omega_n y_{r_2}, \qquad (3.2b)$$

where y_{r1} is the position of the reference path, and y_{r2} its slope. The state equations (3.1) are then augmented with the reference equations (3.2) and the resulting system is written as

$$\dot{x} = Ax + B\delta, \qquad (3.3)$$

where the state vector x is

$$x = \begin{vmatrix} \psi \\ v \\ r \\ y \\ y_{r_1} \\ y_{r_2} \end{vmatrix},$$

and the A, B matrices

$$[A] = \begin{vmatrix} 0 & 0 & 1 & 0 & 0 & 0 \\ 0 & a_{11} & a_{12} & 0 & 0 & 0 \\ 0 & a_{21} & a22 & 0 & 0 & 0 \\ 1 & 1 & 0 & 0 & 0 & 0 \\ 0 & 0 & 0 & 0 & 0 & 1 \\ 0 & 0 & 0 & 0 & -\omega_n^2 & -2\zeta\omega_n \end{vmatrix}$$

$$[B] = \begin{vmatrix} 0 \\ b_1 \\ b_2 \\ 0 \\ 0 \\ 0 \end{vmatrix}$$

C. LINEAR QUADRATIC REGULATOR DESIGN

The LQR method for determining controller gains involves minimizing a cost function in which the integrand is a weighted quadratic function of the state x and the control δ, such as

$$J = \frac{1}{2} \int (e^T Q e + \delta^T R \delta) \, dt ,$$

where T denotes transpose and e is the error in the state of the system; i.e., the difference between actual and reference values. The matrices Q, R represent the different weights in the minimization index J. Large values of R compared to Q result in significant penalization of the control effort and a soft control system. On the other hand, if R is relatively small, the errors in the states are penalized more and the result is increased rudder activity and a tight control system.

In our case we want to minimize the errors in the lateral deviation and the heading between actual and desired vehicles path. Therefore, we use

$$J = \frac{1}{2} \int \left[(y - y_{r_1})^2 + (\psi - y_{r_2})^2 + R\delta^2 \right] dt$$

or

$$J = \frac{1}{2} \int (y^2 + y_{r_1}^2 - 2yy_{r_1} + \psi^2 + y_{r_2}^2 - 2\psi y_{r_2} + R\delta^2) \, dt \ .$$

By looking at this equation the appropriate Q is chosen based on the state equations and is of the form

$$[Q] = \begin{vmatrix} 1 & 0 & 0 & 0 & 0 & -1 \\ 0 & 0 & 0 & 0 & 0 & 0 \\ 0 & 0 & 0 & 0 & 0 & 0 \\ 0 & 0 & 0 & 1 & -1 & 0 \\ 0 & 0 & 0 & -1 & 1 & 0 \\ -1 & 0 & 0 & 0 & 0 & 1 \end{vmatrix}$$

In order to obtain the control gains we must solve the Algebraic Riccatti Equation(ARE) for the positive matrix P

$$A^T P + PA - PBR^{-1}B^T P + Q = 0$$

and the optimal closed loop control is then

$$u = -kx = -R^{-1}B^T Px.$$

The gains k depend on the selection of R. Figure 3.1 shows a plot of the six gains in k versus R, for the values of R ranging from 0.01 to 0.5. It can be seen that the gains become excessively large for R close to 0.01, while they get

very small values for R close to 0.5. A good compromise seems to be about R = 0.1, and this value is therefore selected for the numerical simulations that follow.

With all of the preliminary control work complete, we can now apply our control gains to the following control law

$$\delta = -kx$$

and for our system of equations the control law takes the form

$$\delta = k_1 (\psi - \alpha) + k_2 v + k_3 r + k_4 y + k_5 y_{r_1} + k_6 y_{r_2}$$

We are now ready to analyze our system.
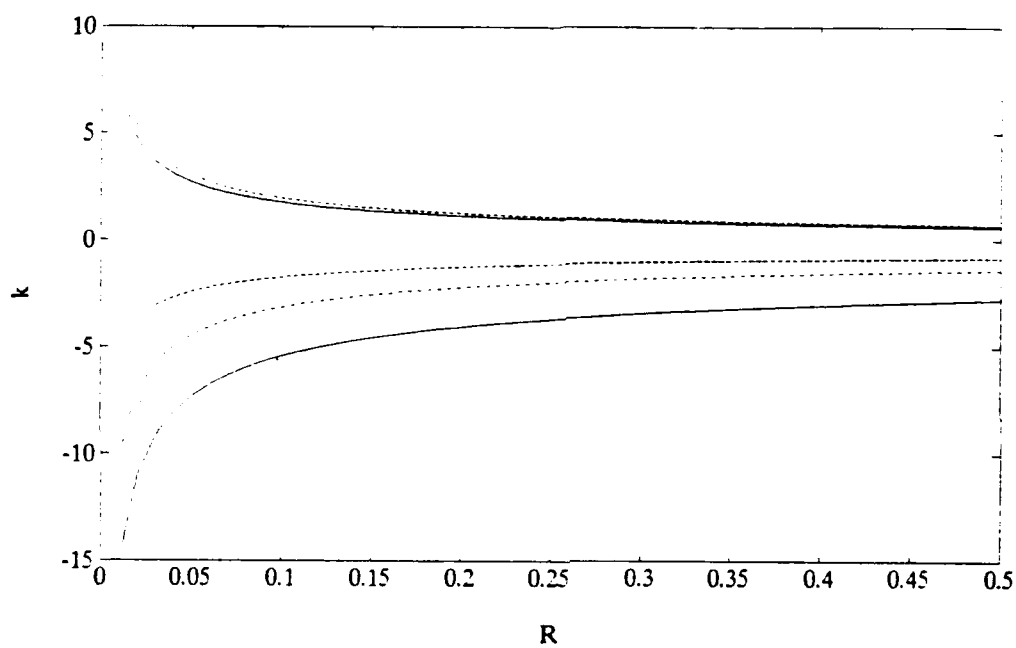
Figure 3.1 k vs R for Values 0.01 to 0.5

19

IV SIMULATION RESULTS

A. INTRODUCTION

Now that the control system has been developed, we must fine tune it in order to insure that the system works properly. A Matlab program was written which first uses a LQR minimization to solve the Algebraic Riccatti Equation for the controller gains and then uses an Euler integration to simulate the response of the control system. The maneuvering of any marine vehicle depends greatly on the advance and transfer characteristics of the vessel. Therefore, the effectiveness of our system depends largely on what distance from the end of a designated path that the vehicle must begin to turn in order to go to the next designated path. This distance is designated as the target distance. First different target distances are looked at for one angle α. Then the chosen target distance is applied to a variety of angles to ensure conformity.

B. TARGET DISTANCE SELECTION

By using $\alpha = 45°$, target distances ranging from 1.0 to 4.0 shiplengths were used in increments of 0.5. For each target distance three separate qualifiers were looked at in order to determine the effectiveness of the system. These were the

global path, which showed that the system was traveling the desired smooth path, the local path, which showed how the vehicle was following the reference path, and the rudder angle, which gave indications of how hard the mechanical system had to work.

For an $\alpha = 45°$ and a target distance = 1.0 we found that the system would overshoot the path and had difficulty following the reference path (figures 4.1 and 4.2). In addition, figure 4.3 shows that the mechanical system would have to work very hard to try and keep the vehicle on track. Figures 4.4 and 4.7 show that for an $\alpha = 45°$ and target distances of 1.5 and 2.0 the system would produce a smooth path that that was smooth in nature and close to the desired path. However, the local path showed that the actual track was not following the reference path closely (figures 4.5 and 4.8). Figures 4.6 and 4.9 show the rudder movement of the system, indicating that the system must still work hard to maintain the path.

As we moved to larger values of target distance, the actual path and the reference path moved closer to each other. Local paths could be generated that where almost on top of each other. This basically held true for all of the values beyord the 2.5 shiplength target distance, however, for the 3.5 and 4.0 target distance, it was found that the global path would stray from the original path (figures 4.10 thru 4.15). This is attributed to the fact that the reference path is

being generated too far away from the new track and too much of the second order reference path was generated. After carefully looking at these graphs, it seemed that the best choice for a target distance would be the 2.5 shiplengths (figures 4.16 thru 4.18). This distance seemed to provide the optimum performance of the control system by producing the desired smooth path, with accurate path following, and not overworking of the mechanical system.

C. APPLICATION

Now that a target of 2.5 has been chosen, all angles in the quadrant were observed to ensure that the selected target distance would perform for all angles (figures 4.19 thru 4.42). It was found that the 2.5 shiplength target distance would work satisfactorily for all of the angles in the quadrant. The desired smooth path was produced while the track followed closely to the reference path. It seems that the only possible draw back to using the constant target distance is the work of the mechanical system. As we move to the higher angles, the system must max out the rudder for longer periods of time. In comparison this is a relatively short period of time and should not pose a problem.
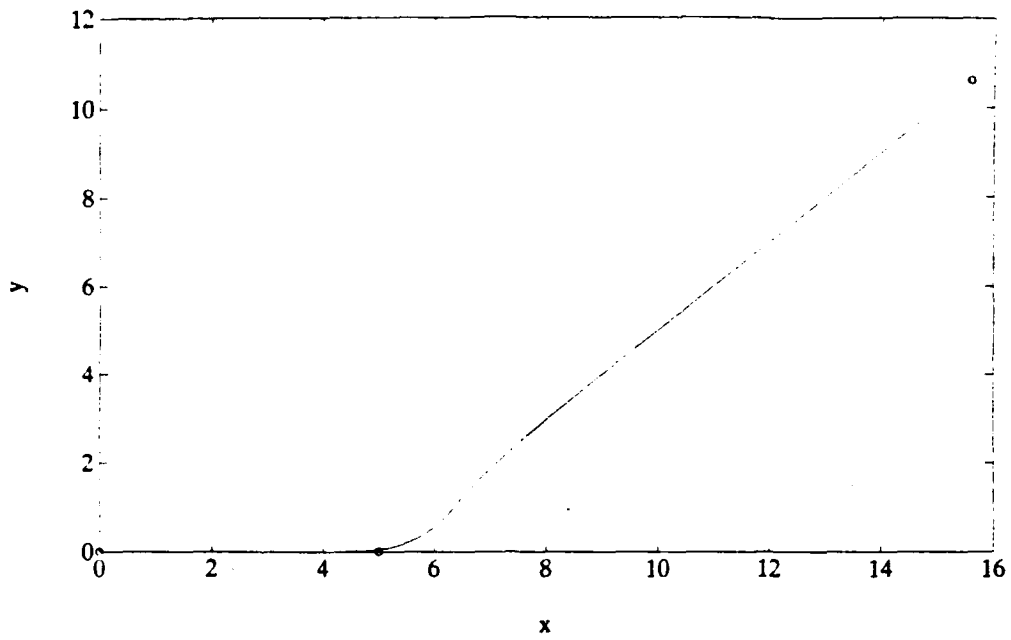
Figure 4.1 Global Path for $\alpha = 45°$ and Target Distance = 1.0
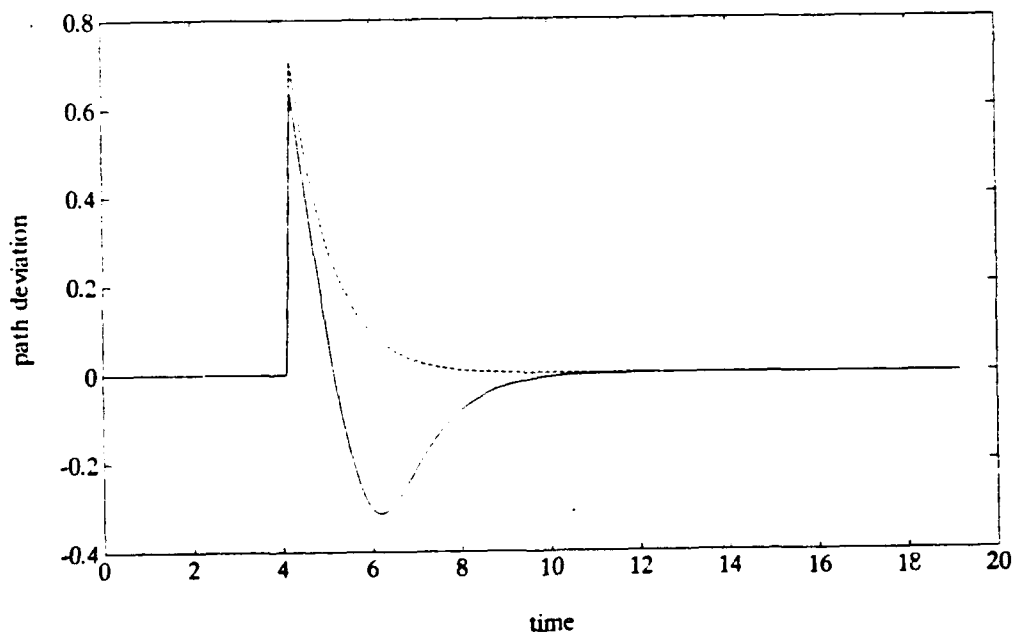
Figure 4.2 Local Path for $\alpha = 45°$ and Target Distance = 1.0
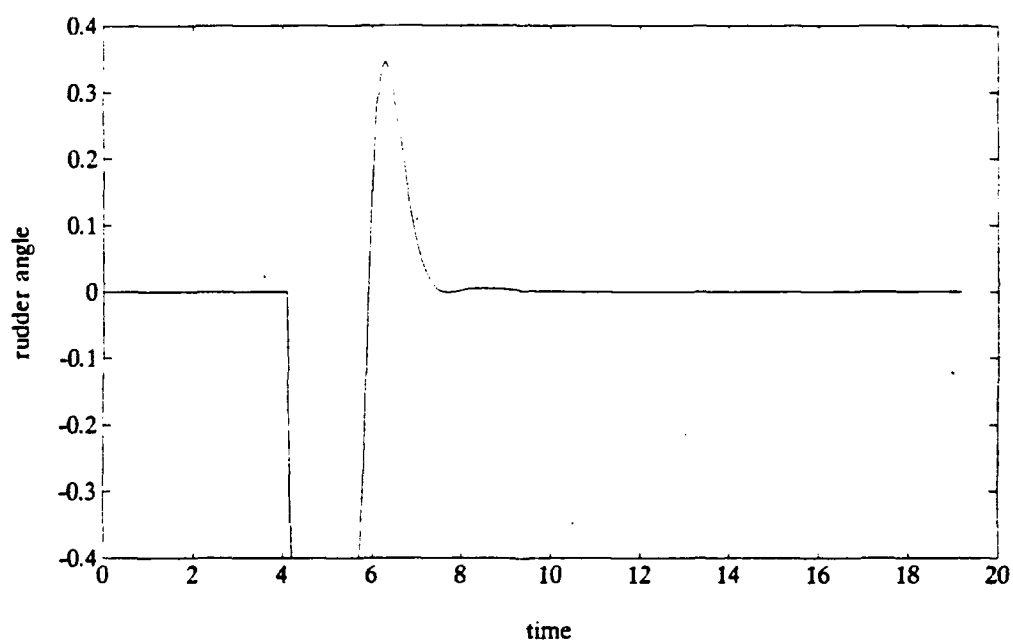
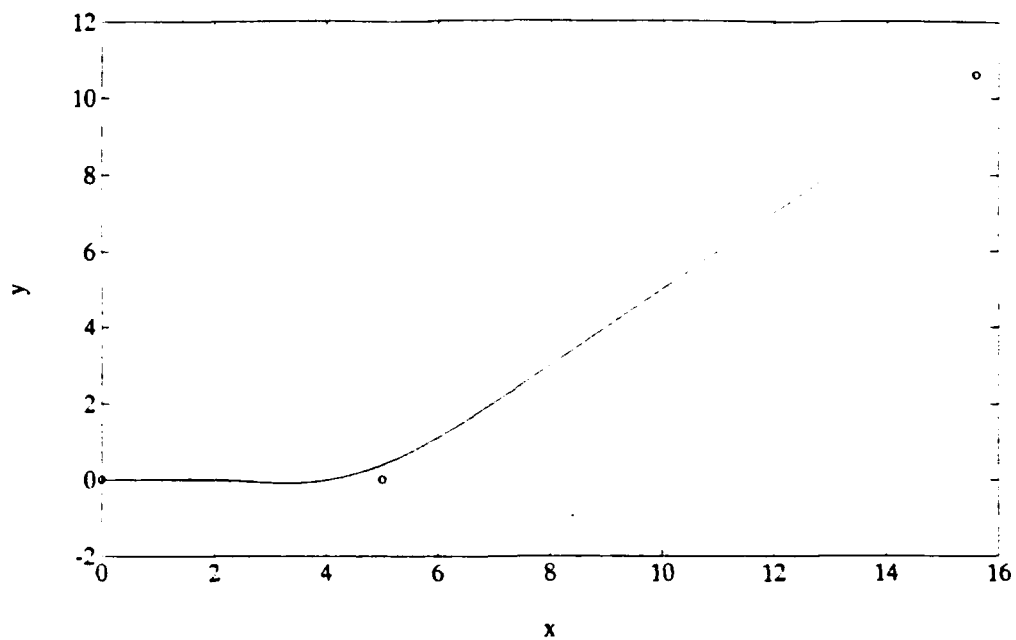Figure 4.3 Rudder Angle for $\alpha = 45°$ and Target Distance=1.0
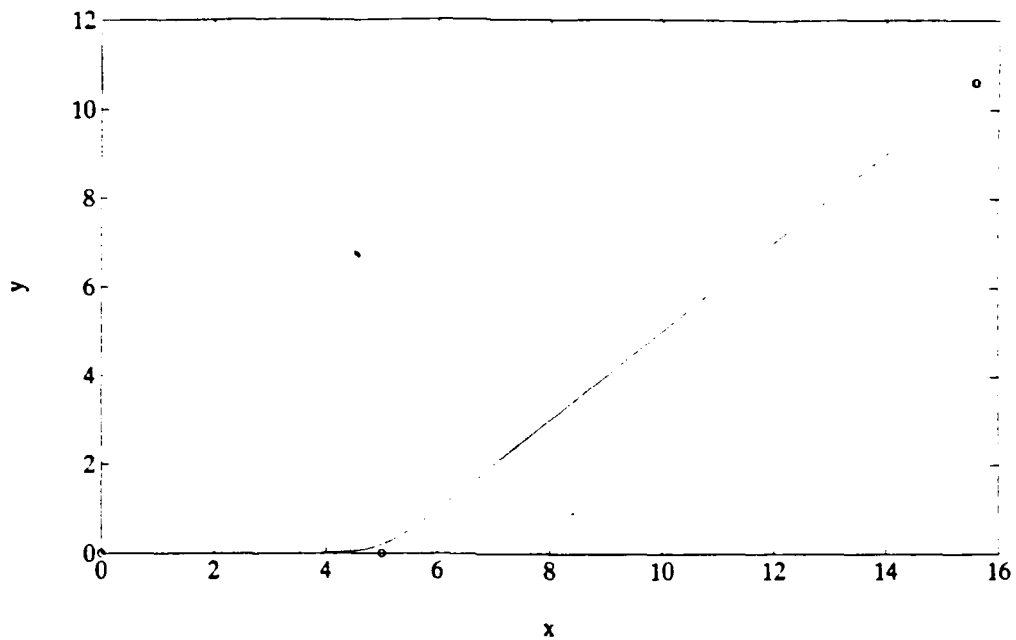
Figure 4.4 Global Path for $\alpha = 45°$ and Target Distance = 1.5
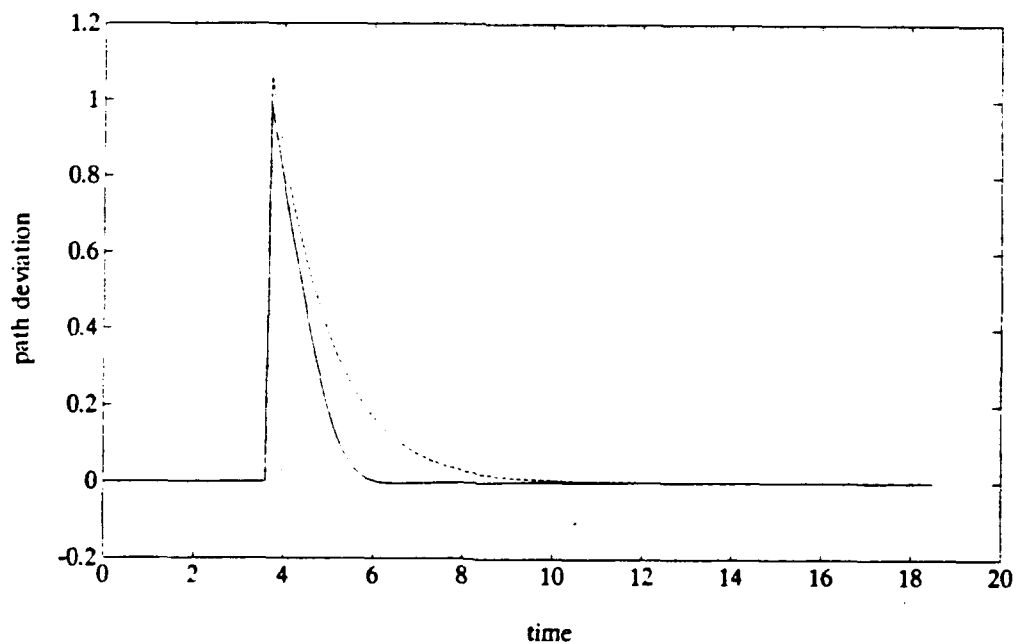
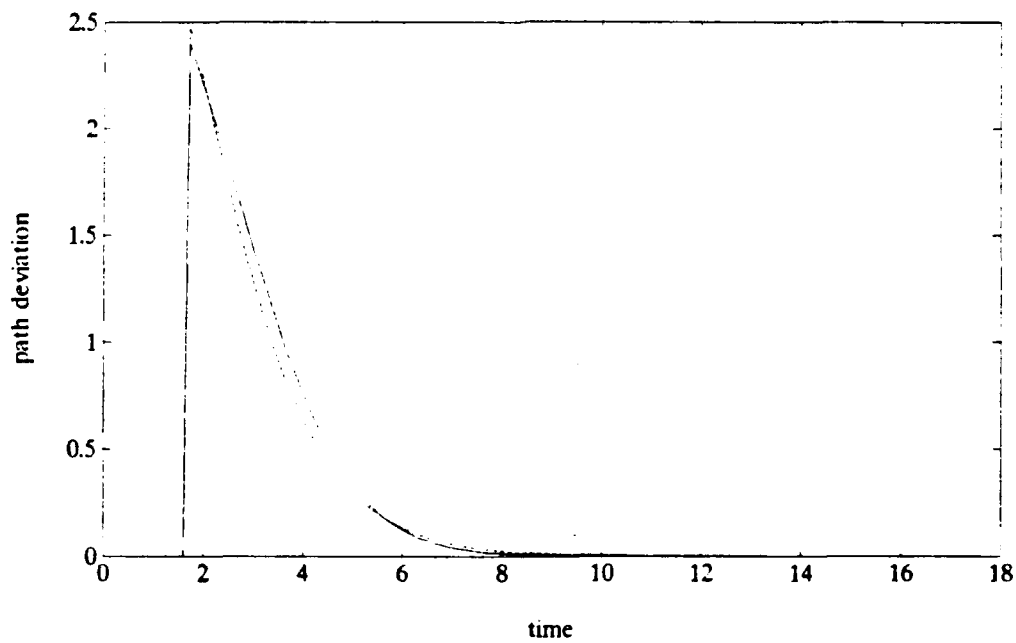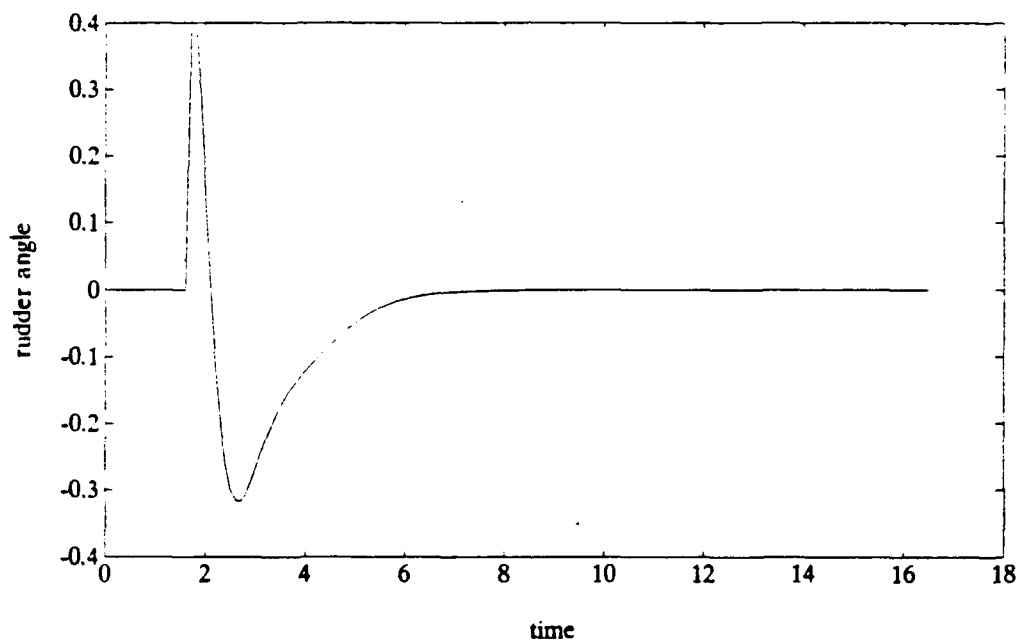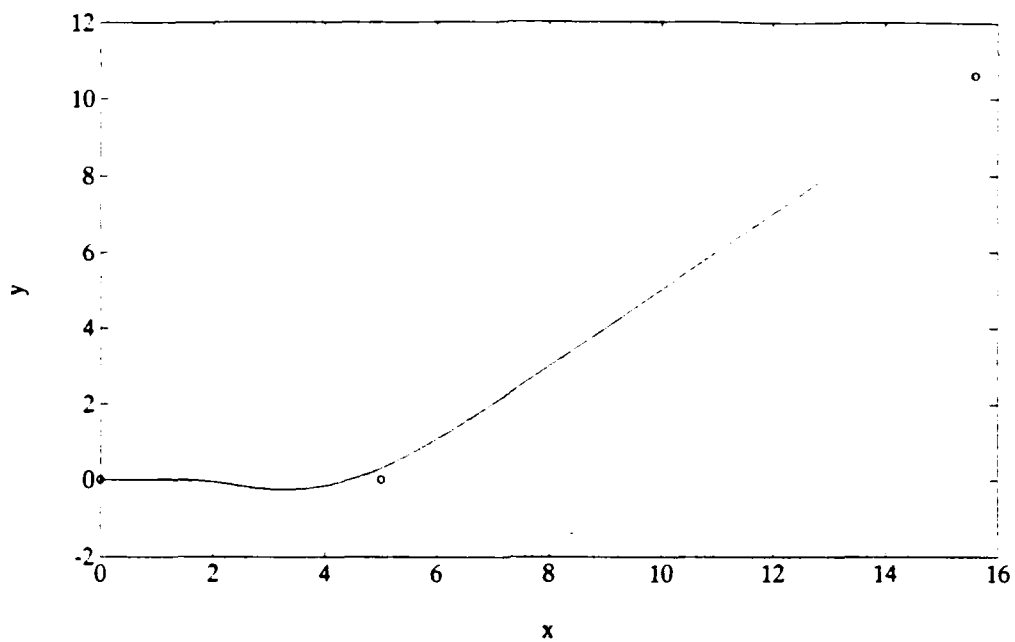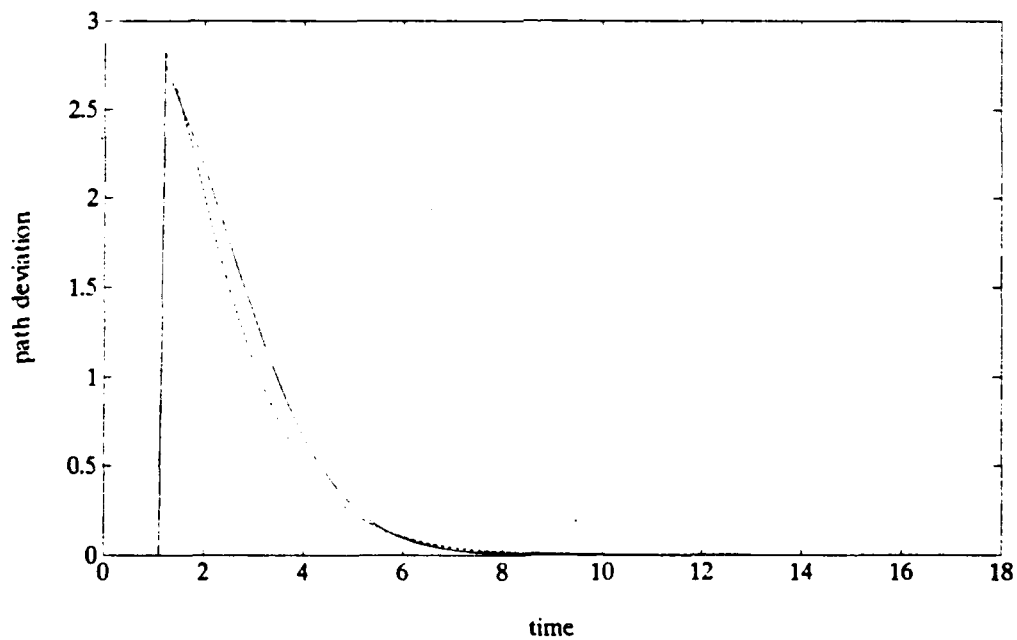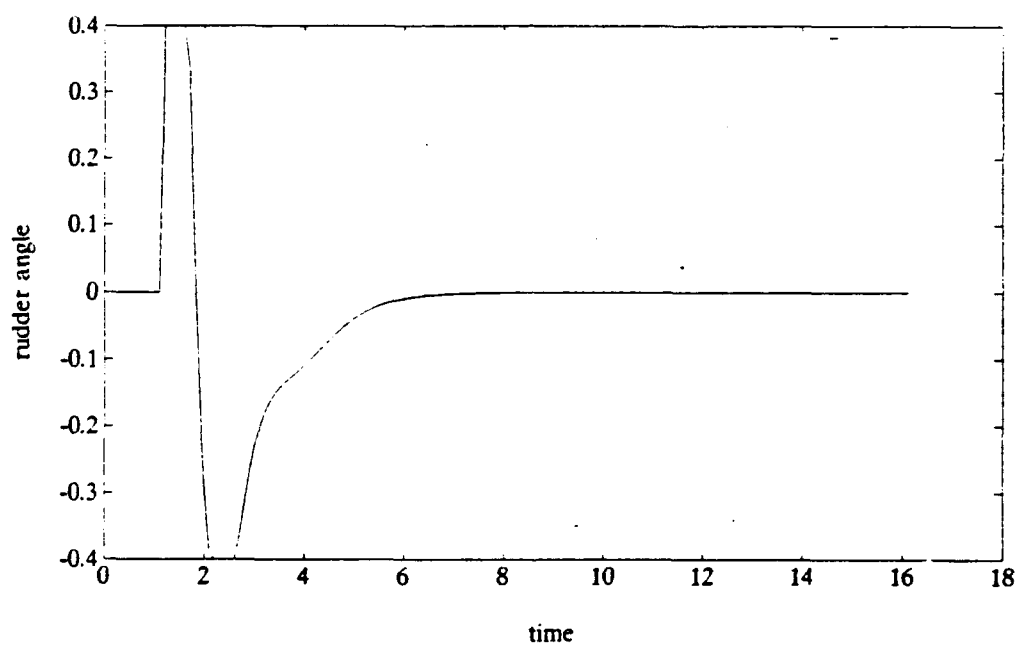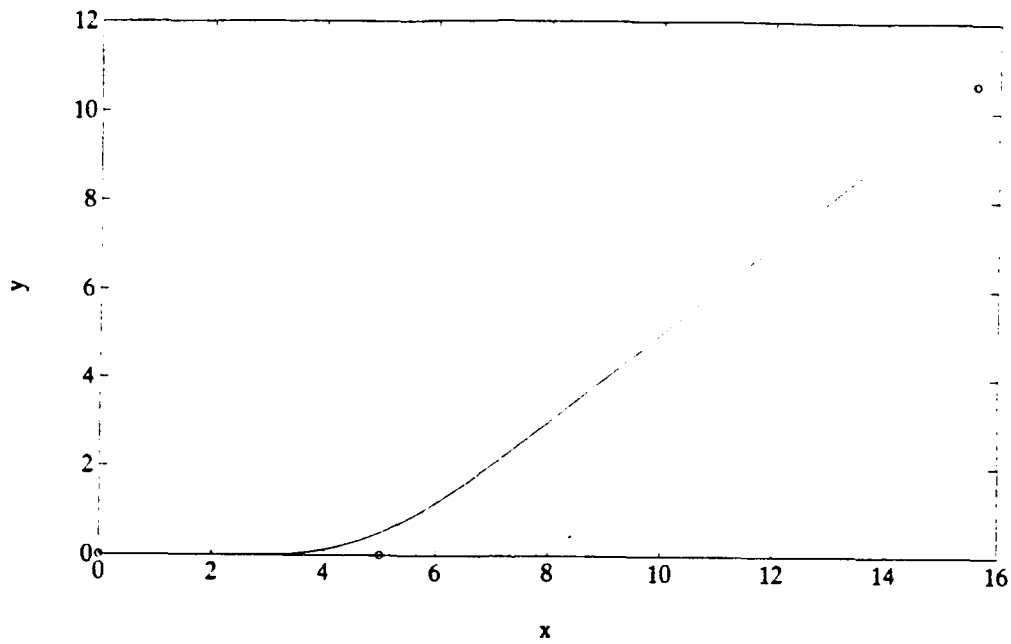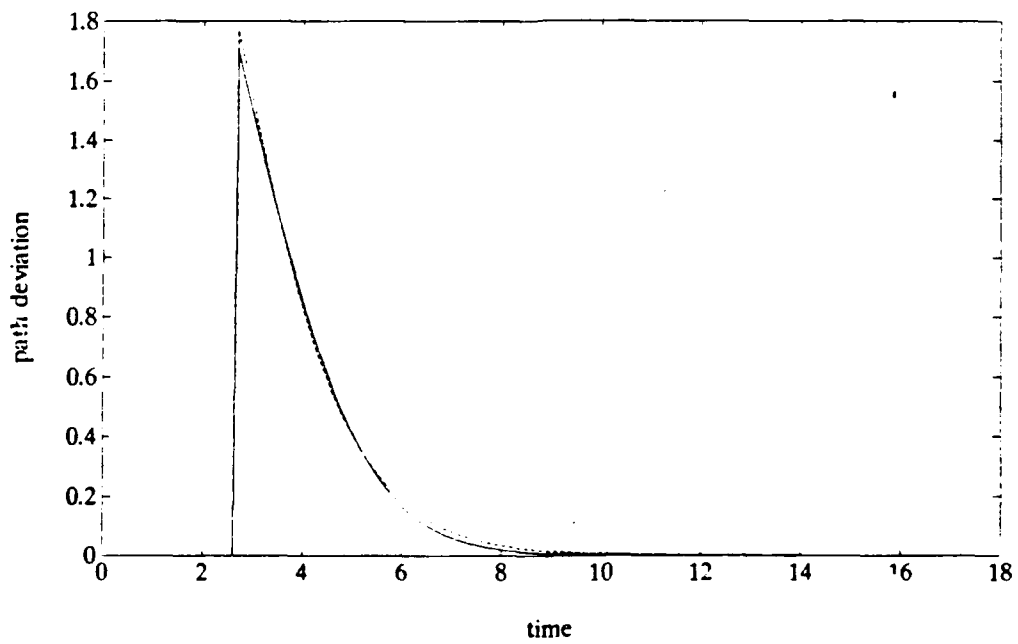Figure 4.5 Local Path for $\alpha = 45°$ and Target Distance = 1.5
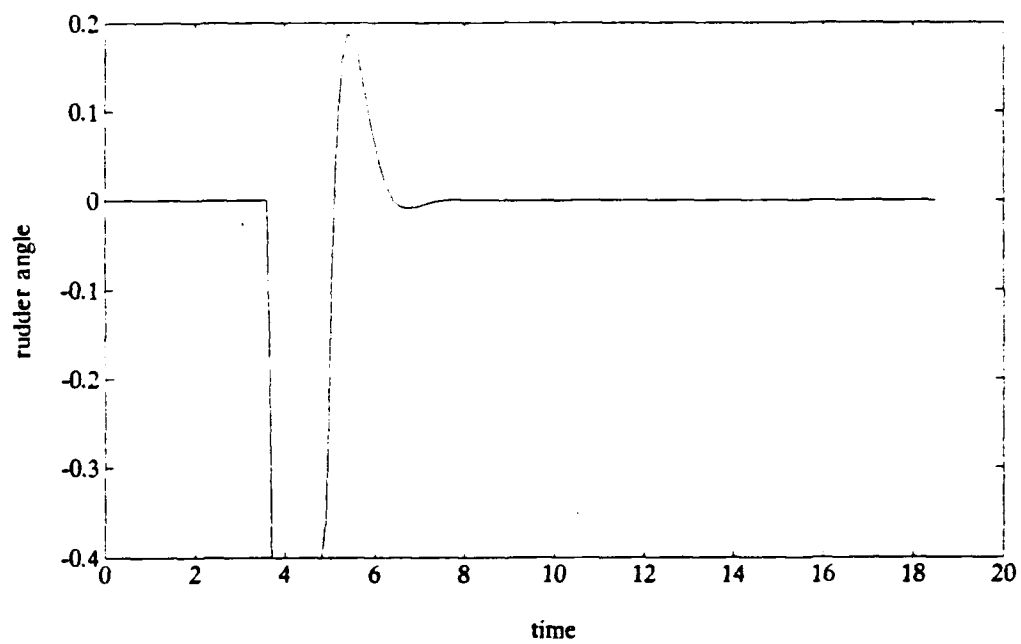
Figure 4.6 Rudder Angle for $\alpha = 45°$ and Target Distance $=1.5$
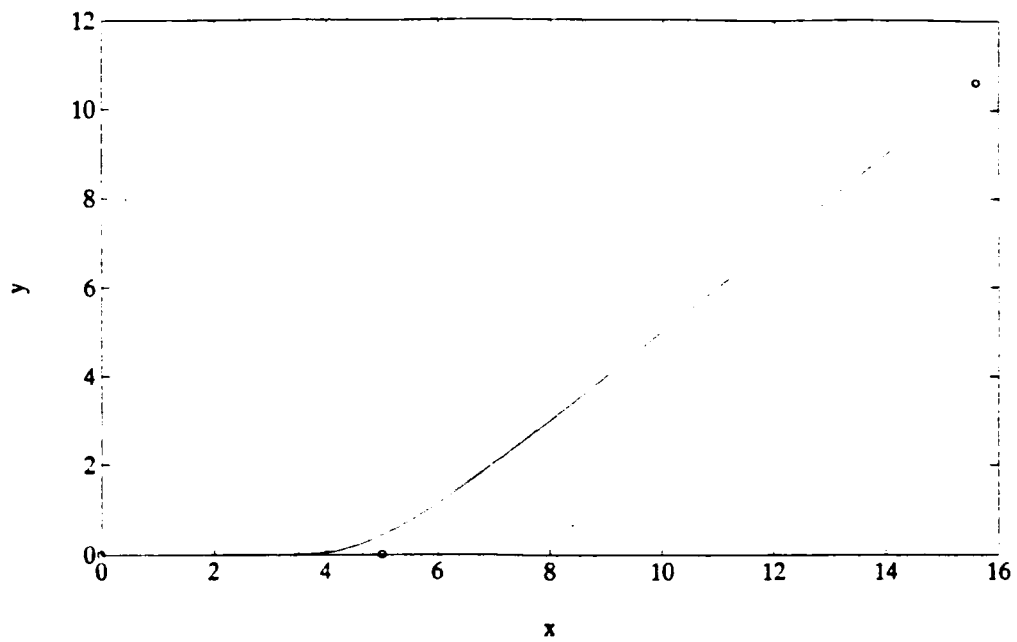
Figure 4.7 Global Path for α = 45° and Target Distance = 2.0
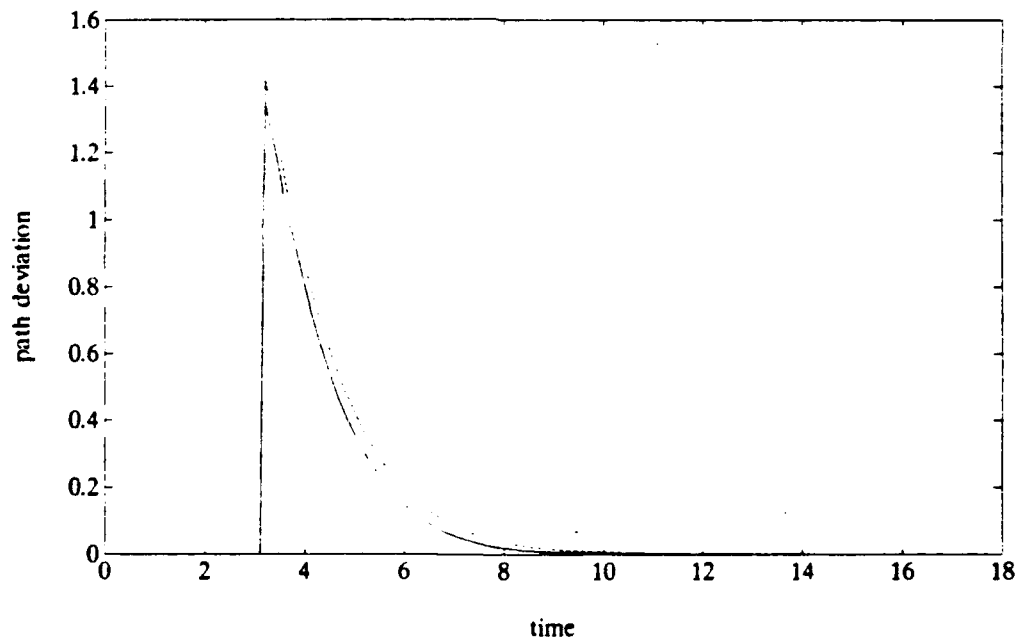
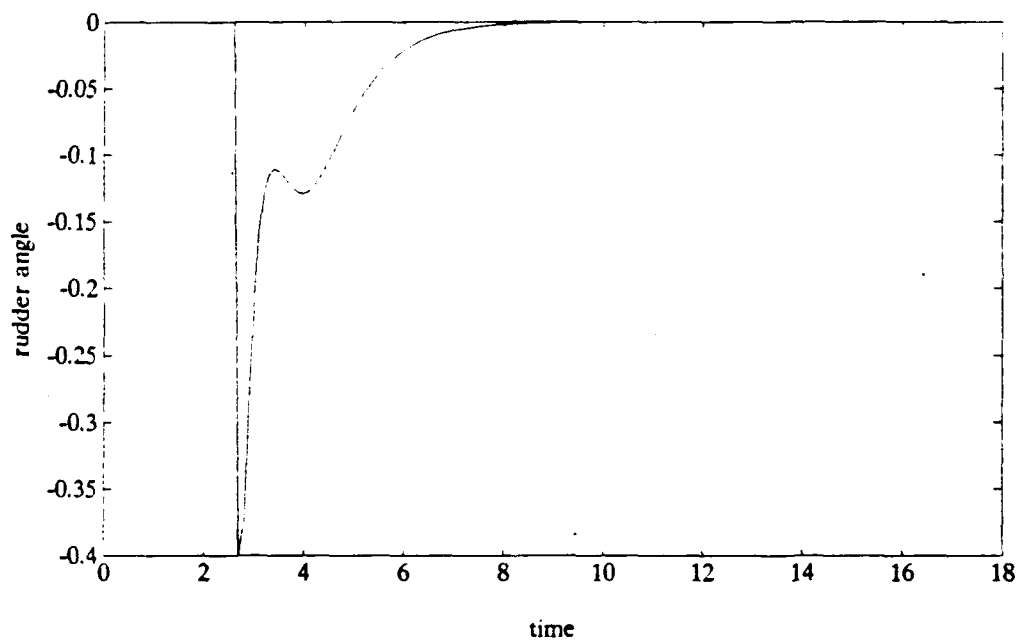Figure 4.8 Local Path for α = 45° and Target Distance = 2.0
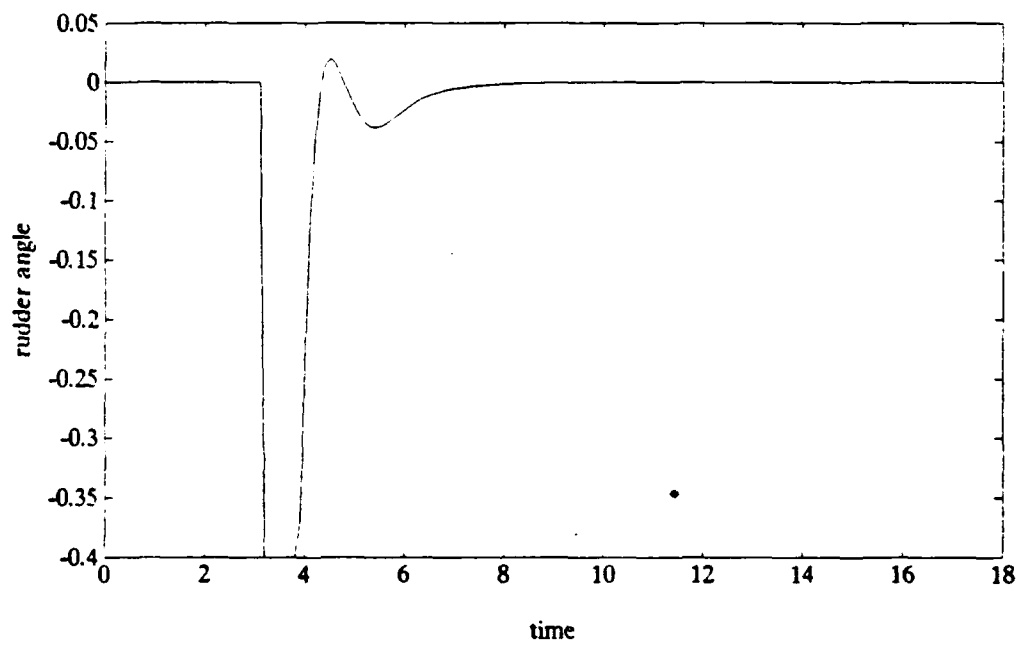
Figure 4.9 Rudder Angle for $\alpha = 45°$ and Target Distance $=2.0$

Figure 4.10 Global Path for α = 45° and Target Distance =3.5

Figure 4.11 Local Path for α = 45° and Target Distance = 3.5

29

Figure 4.12 Rudder Angle for $\alpha = 45°$ and Target Distance=3.5

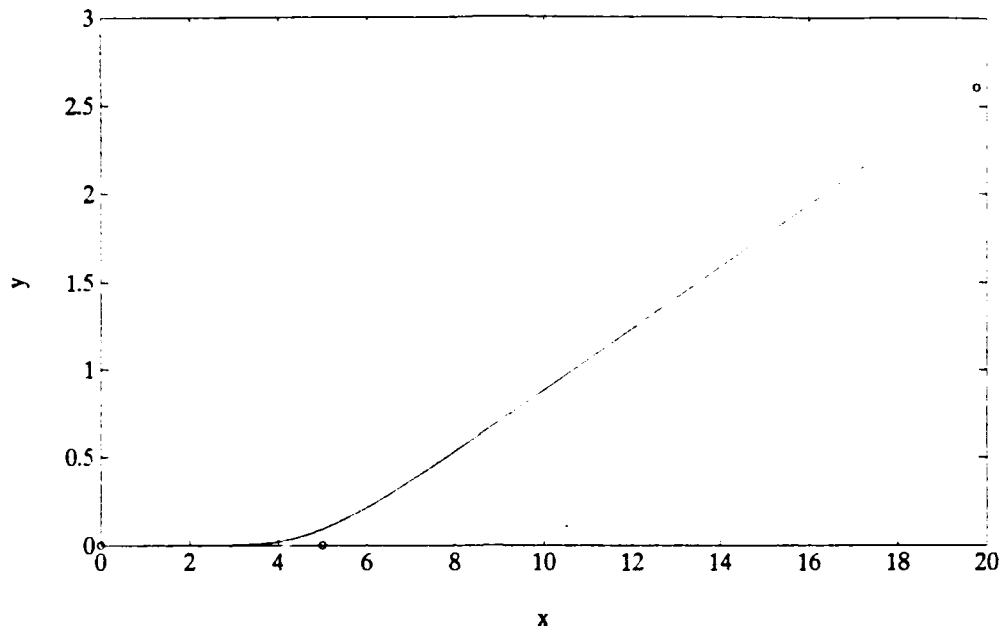Figure 4.13 Global Path for α = 45° and Target Distance =4.0
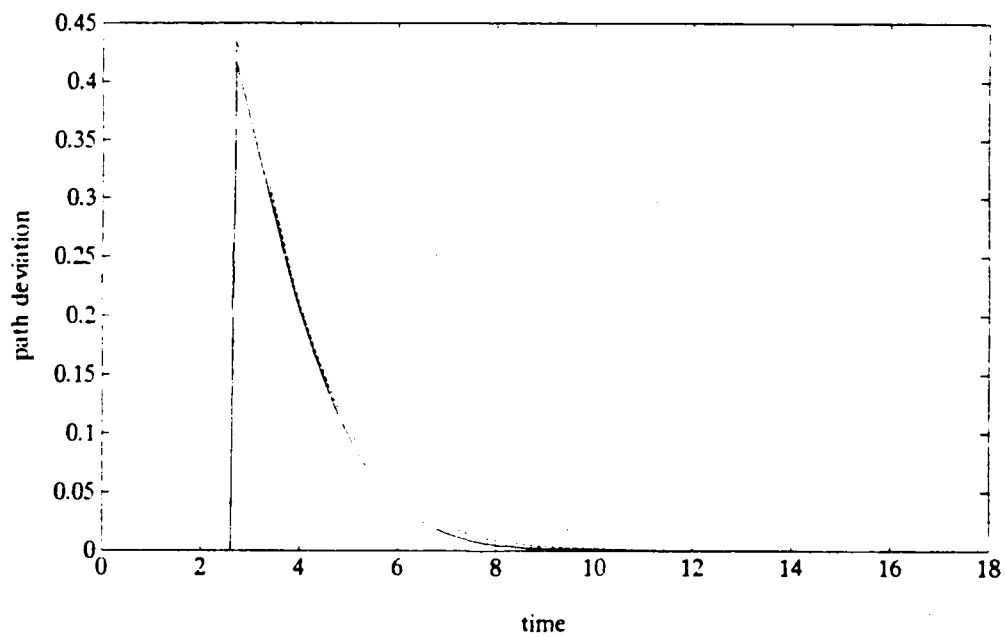

Figure 4.14 Local Path for α = 45° and Target Distance = 4.0

31

Figure 4.15 Rudder Angle for $\alpha = 45°$ and Target Distance=4.0

Figure 4.16 Global Path for α = 45° and Target Distance =2.5

Figure 4.17 Local Path for α = 45° and Target Distance = 2.5

33

Figure 4.18 Rudder Angle for α = 45° and Target Distance=2.5

Figure 4.19 Global Path for $\alpha = 10°$
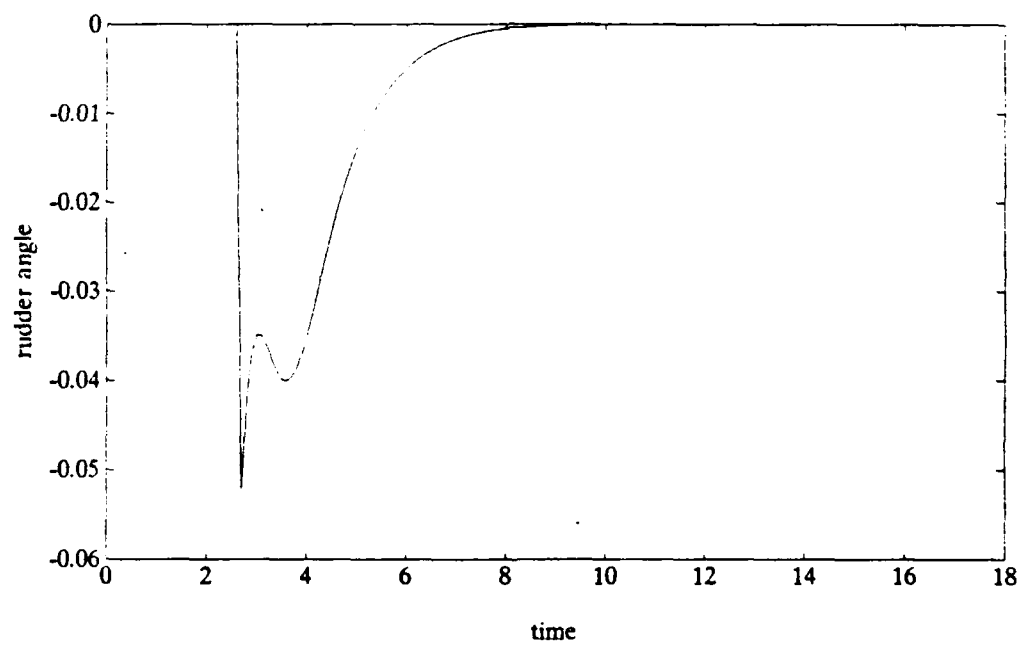

Figure 4.20 Local Path for $\alpha = 10°$

35

Figure 4.21 Rudder angle for α = 10°
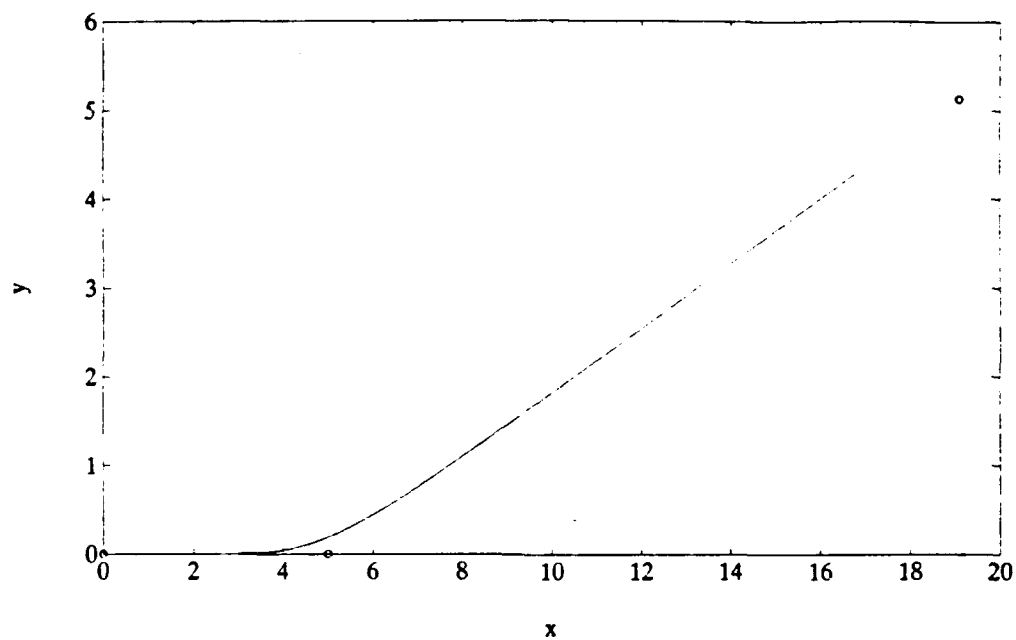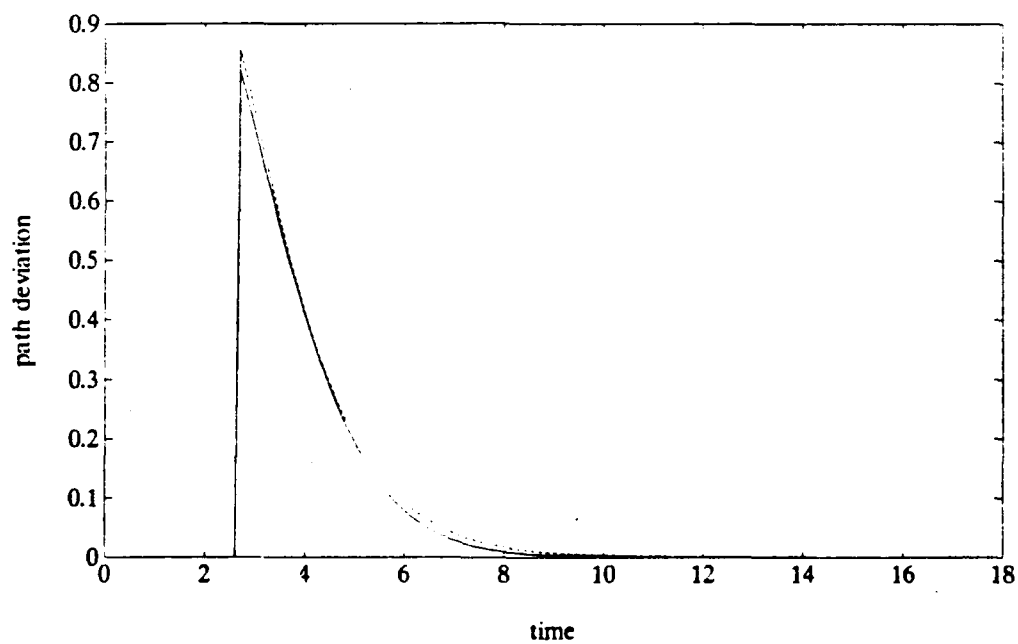
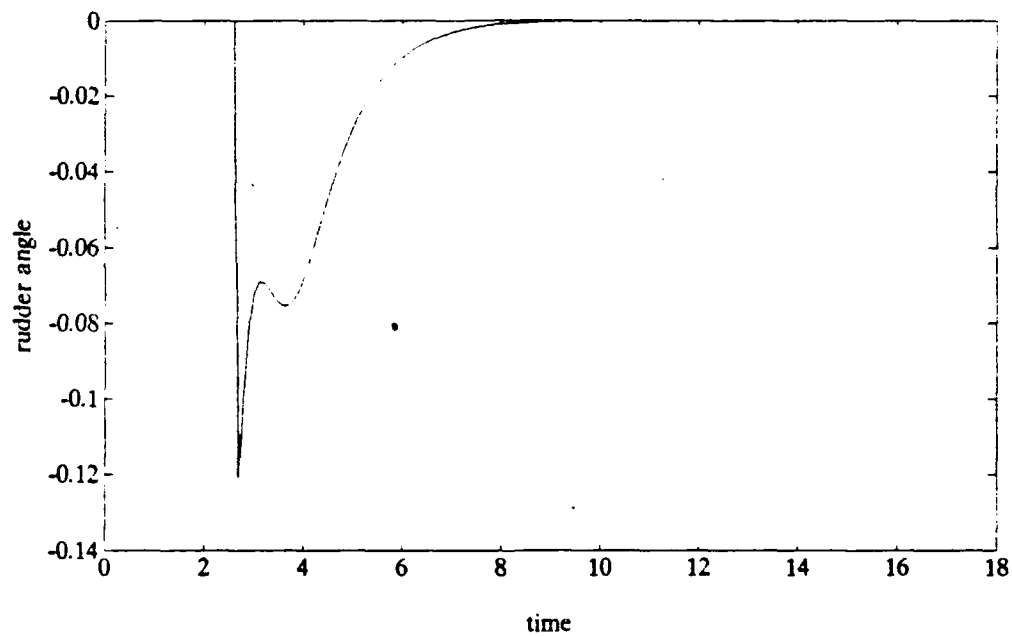Figure 4.22 Global Path for α = 20°

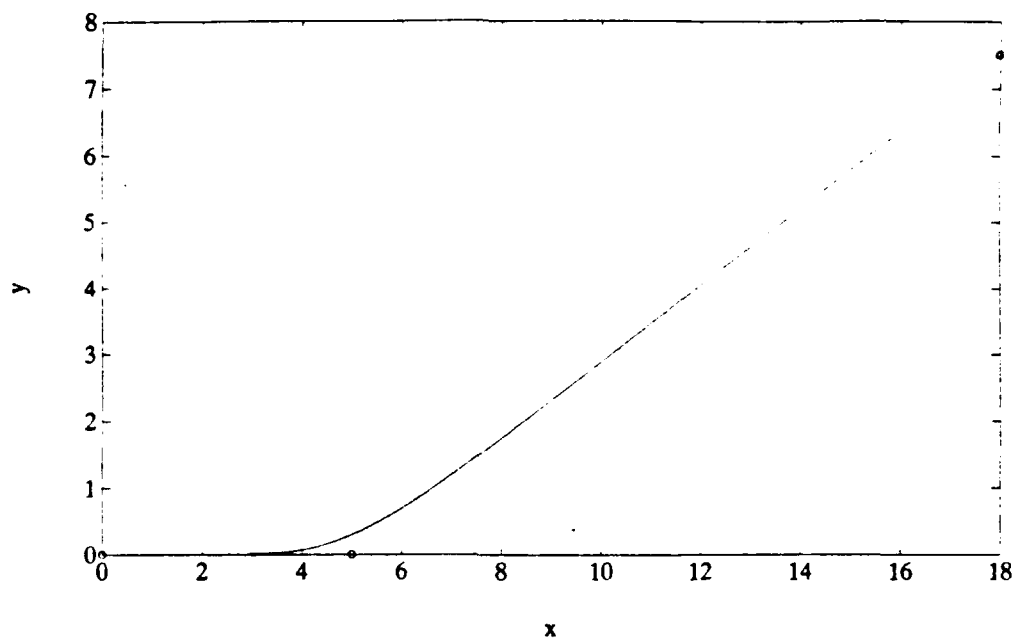Figure 4.23 Local Path for α = 20°

Figure 4.24 Rudder Angle for $\alpha = 20°$

Figure 2.25 Global Path for $\alpha = 30°$

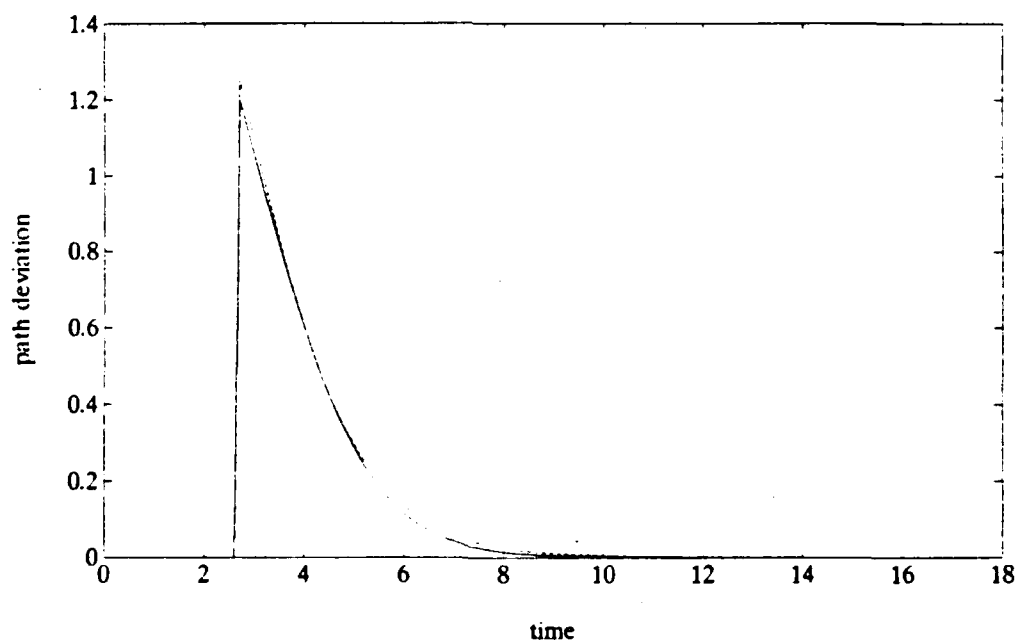Figure 4.26 Local Path for $\alpha = 30°$
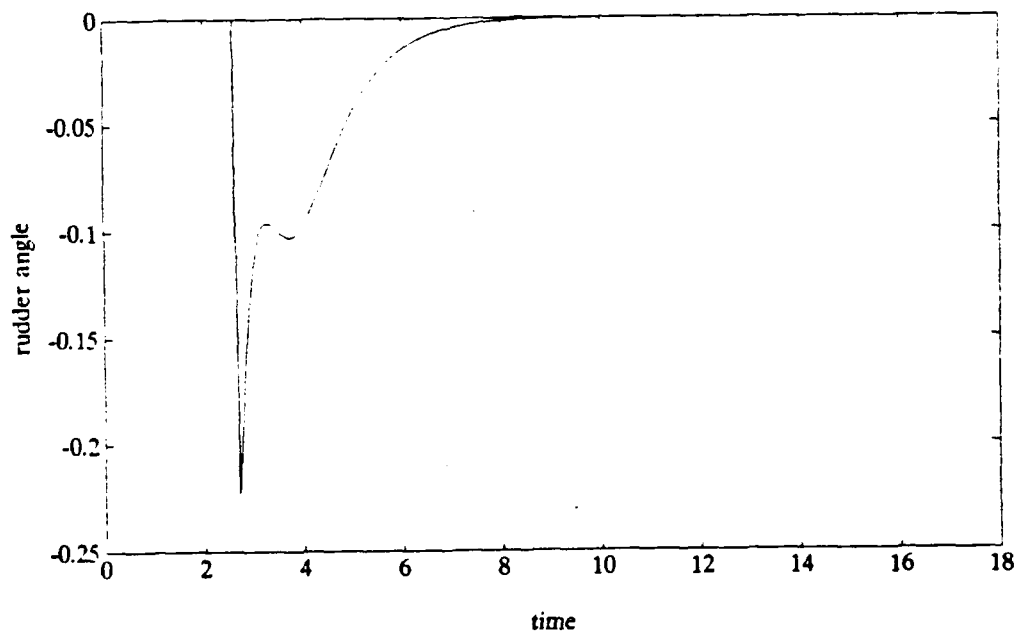
Figure 4.27 Rudder Angle for α = 30°

Figure 4.28 Global Path for α = 40°

Figure 4.29 Local Path for α = 40°

41

Figure 4.30 Rudder Angle for $\alpha = 40°$

Figure 4.31 Global Path for $\alpha = 50°$

Figure 4.32 Local Path for $\alpha = 50°$

Figure 4.33 Rudder Angle for $\alpha = 50°$

Figure 4.34 Global Path for $\alpha = 60°$
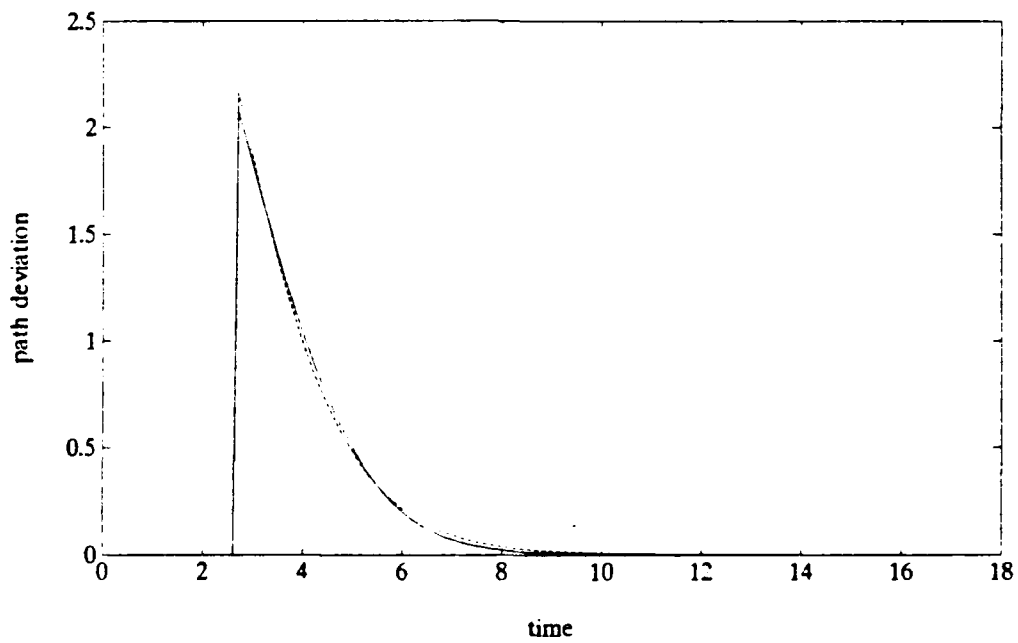
Figure 4.35 Local Path for $\alpha = 60°$
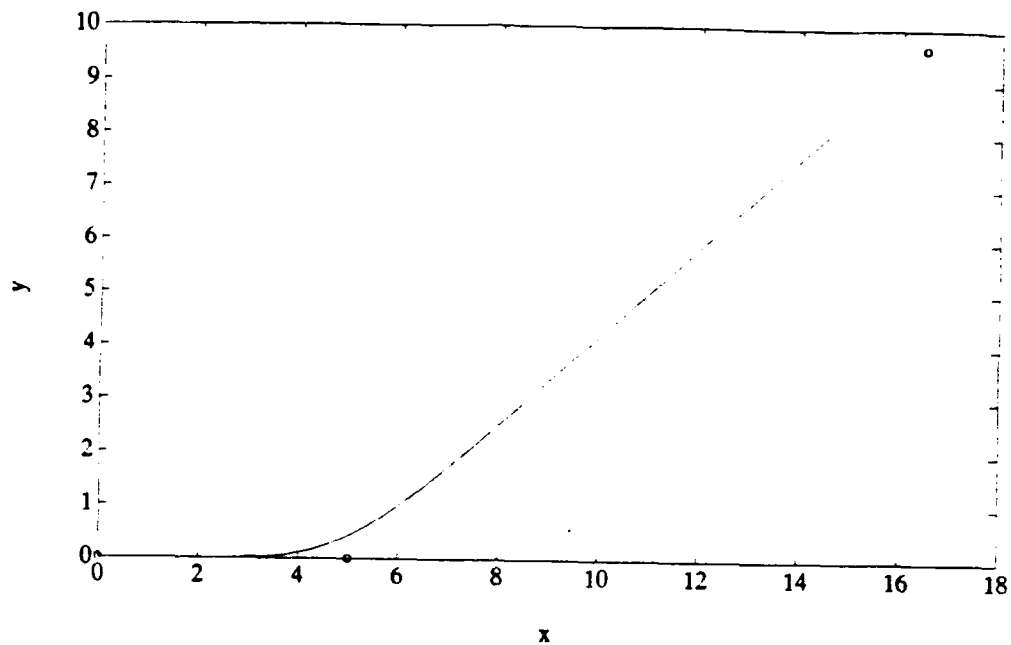
45
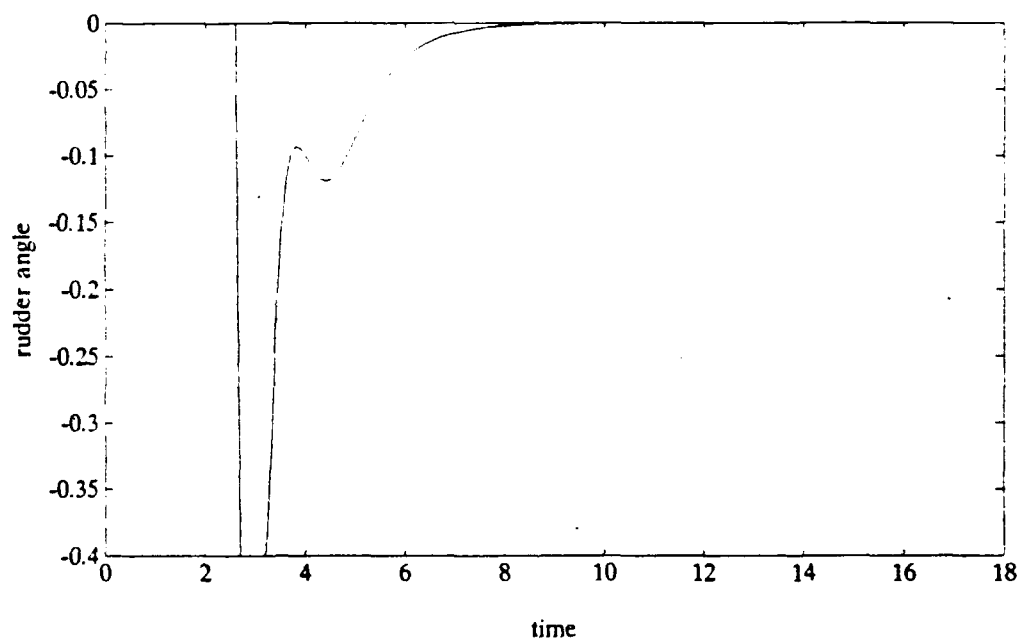
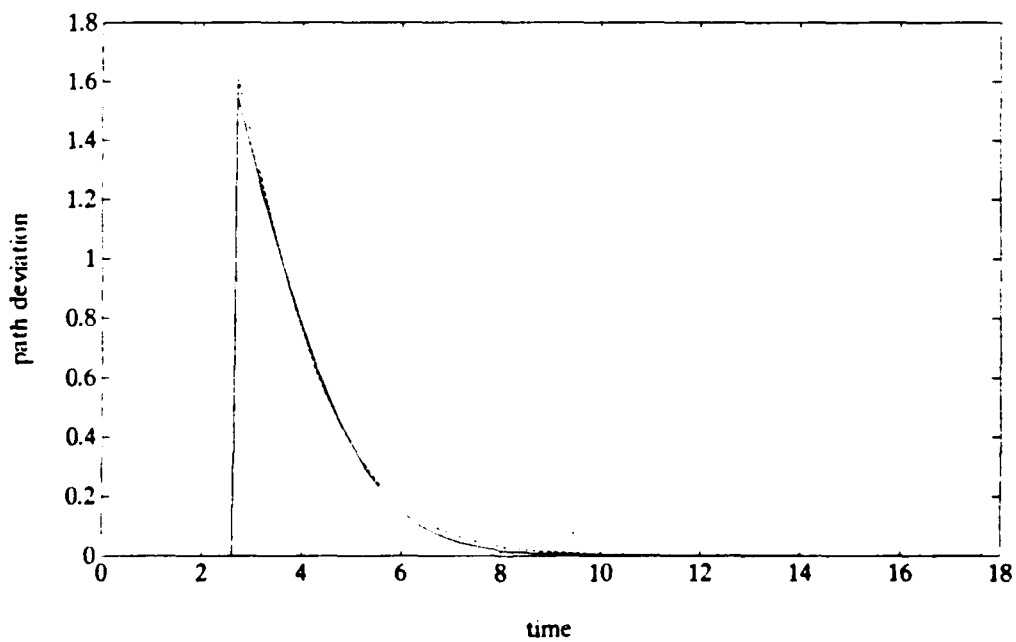Figure 4.36 Rudder Angle for α = 60°
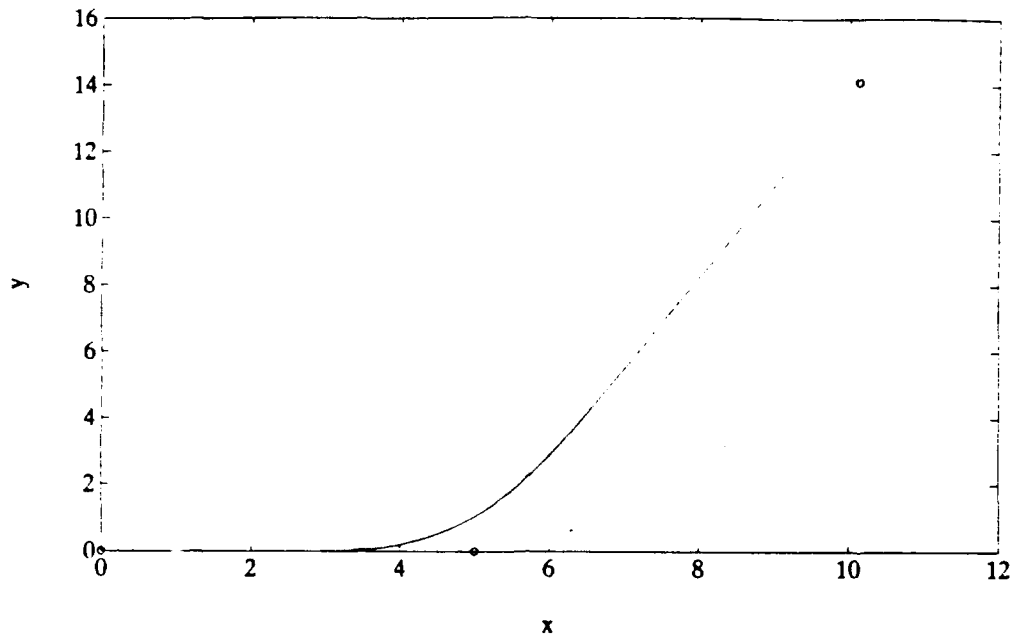
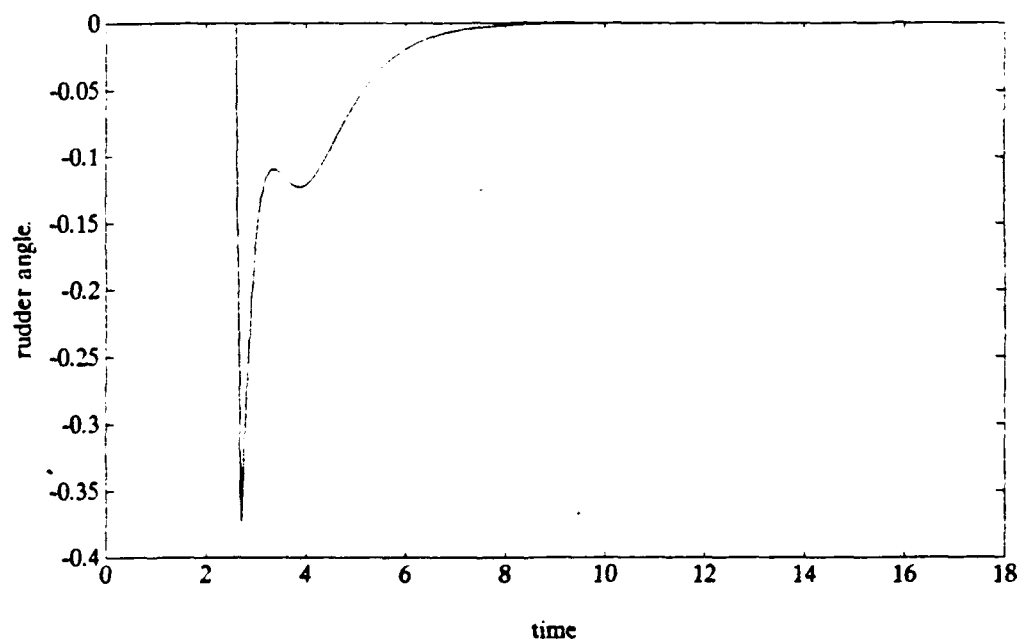Figure 4.37 Global Path for $\alpha = 70°$
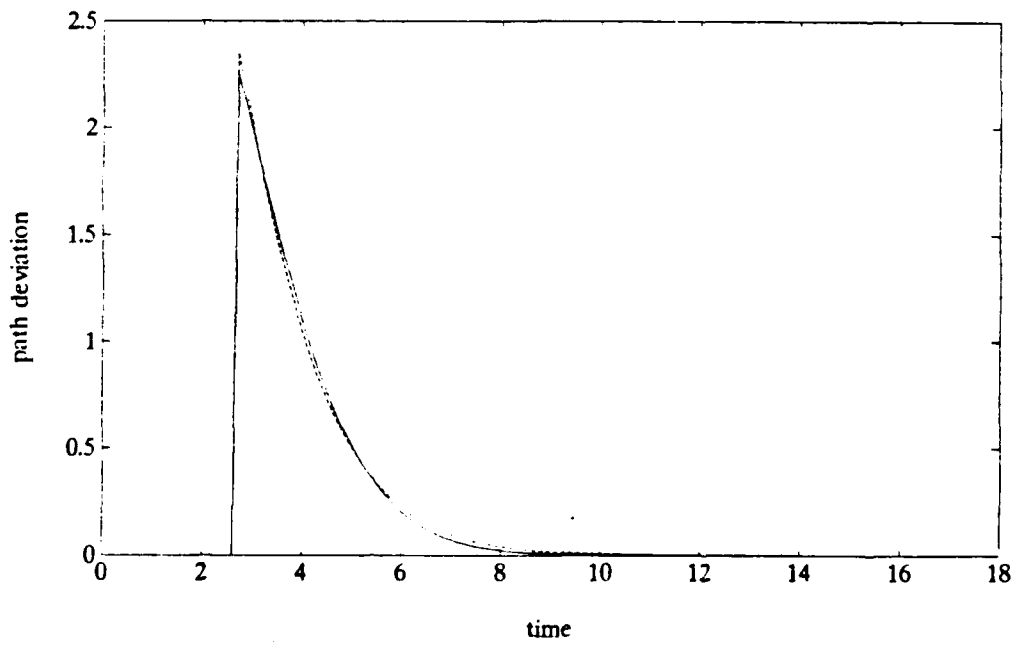
Figure 4.38 Local Path for $\alpha = 70°$
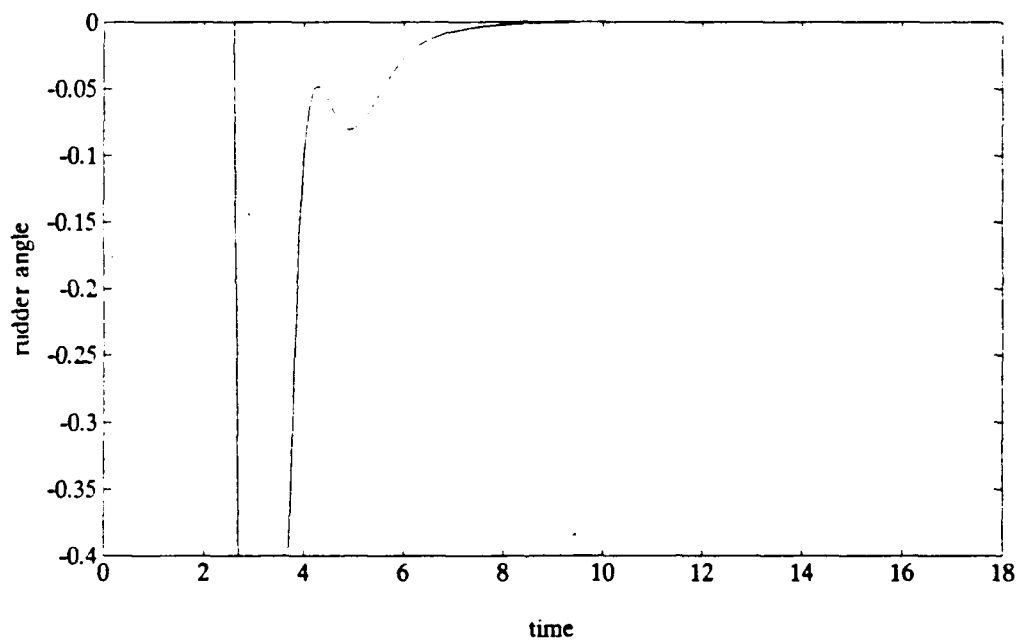
Figure 4.39 Rudder Angle for $\alpha = 70°$
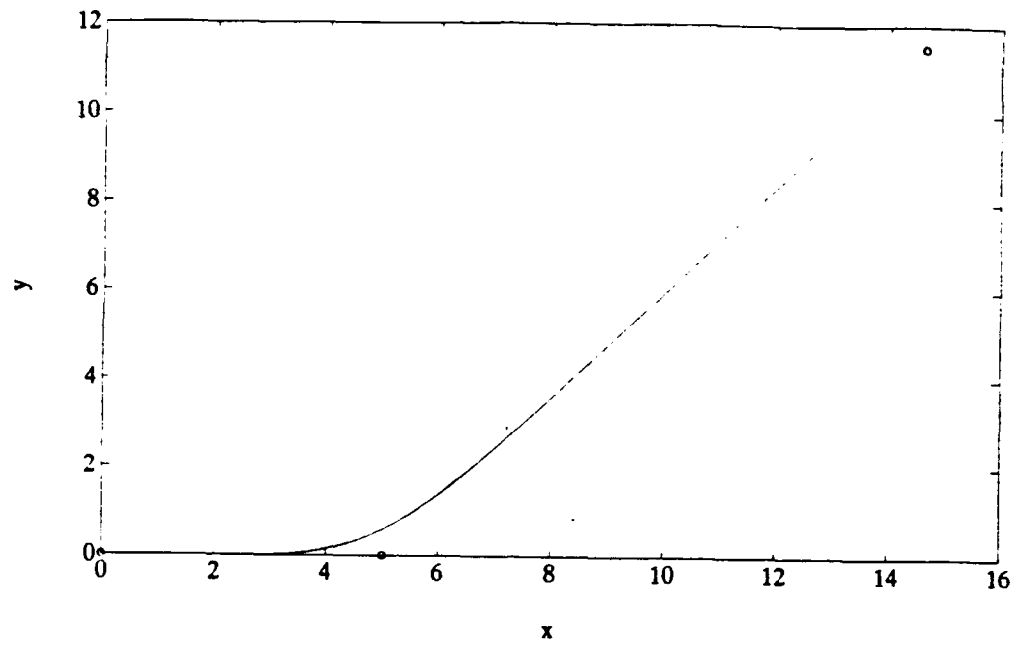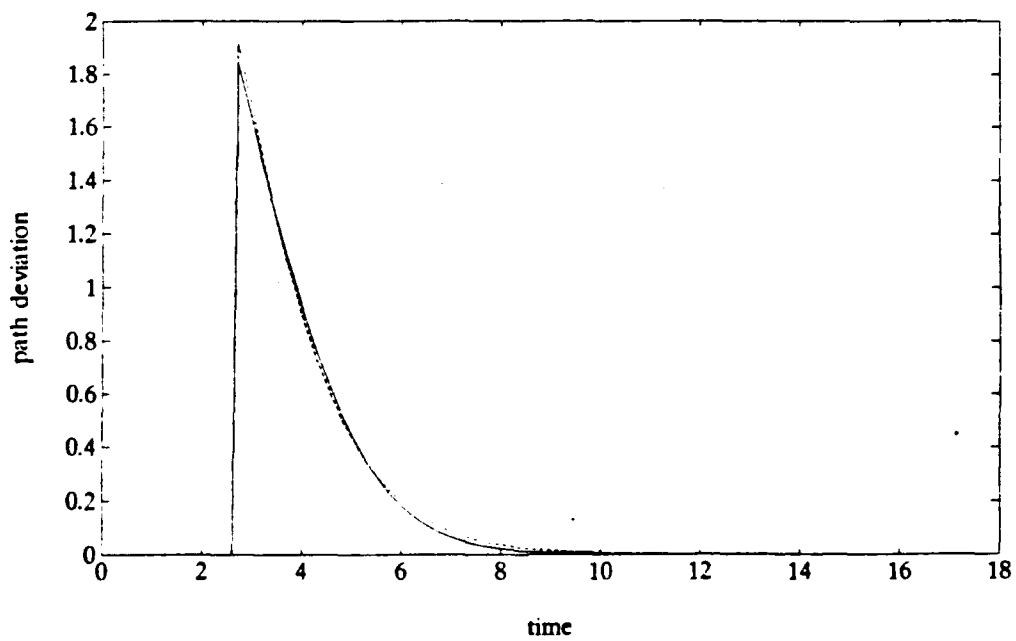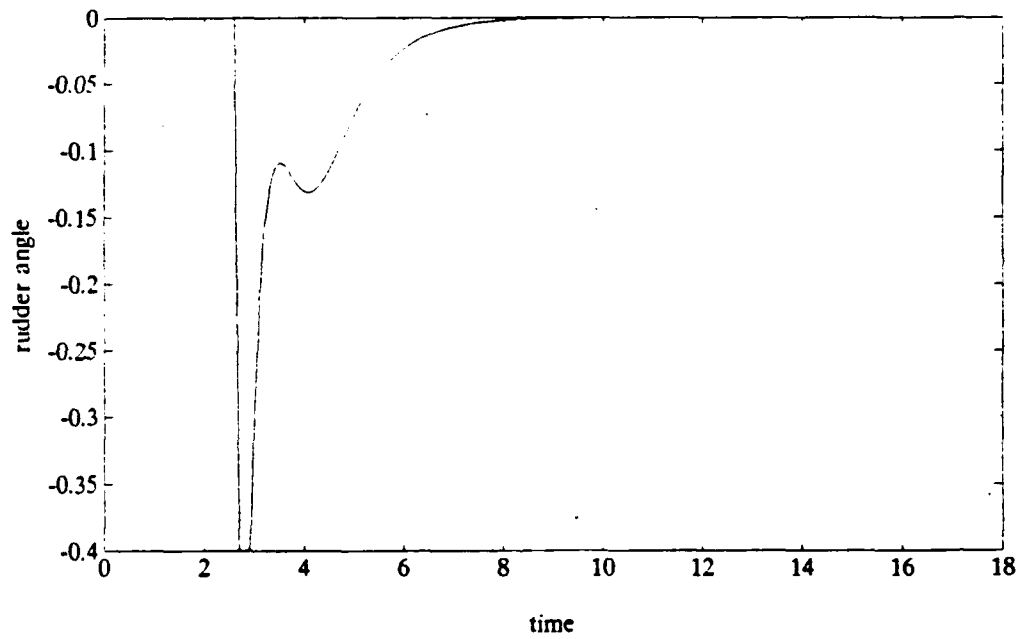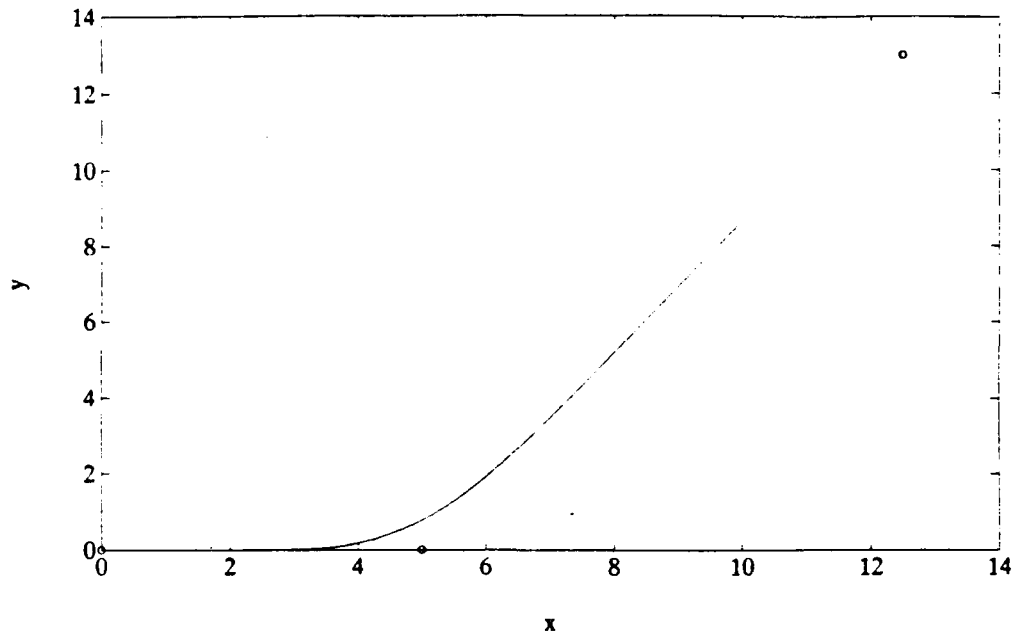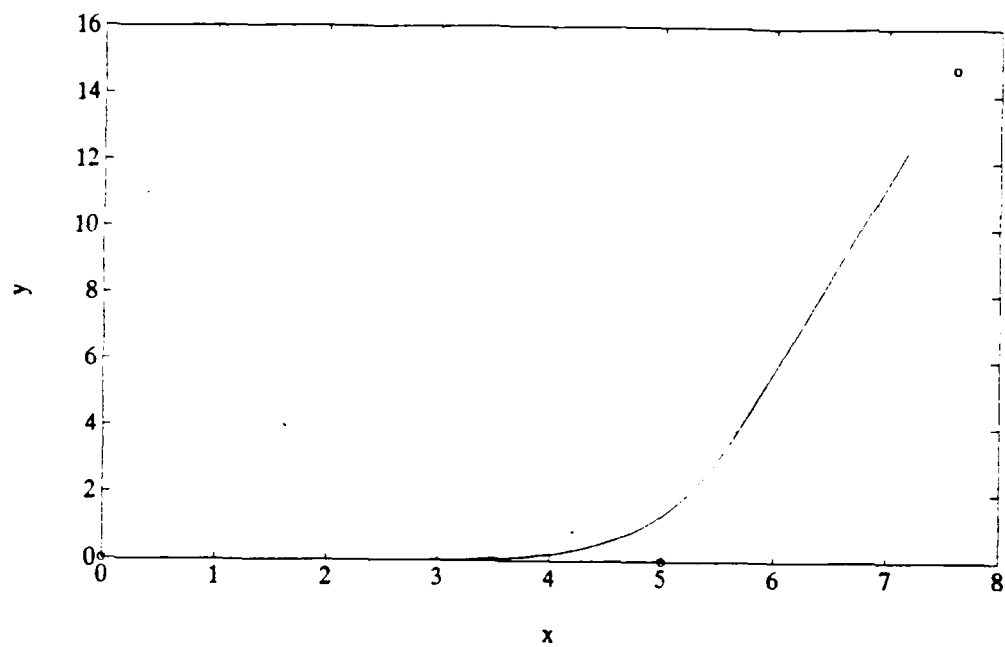
Figure 4.40 Global Path for $\alpha = 80°$
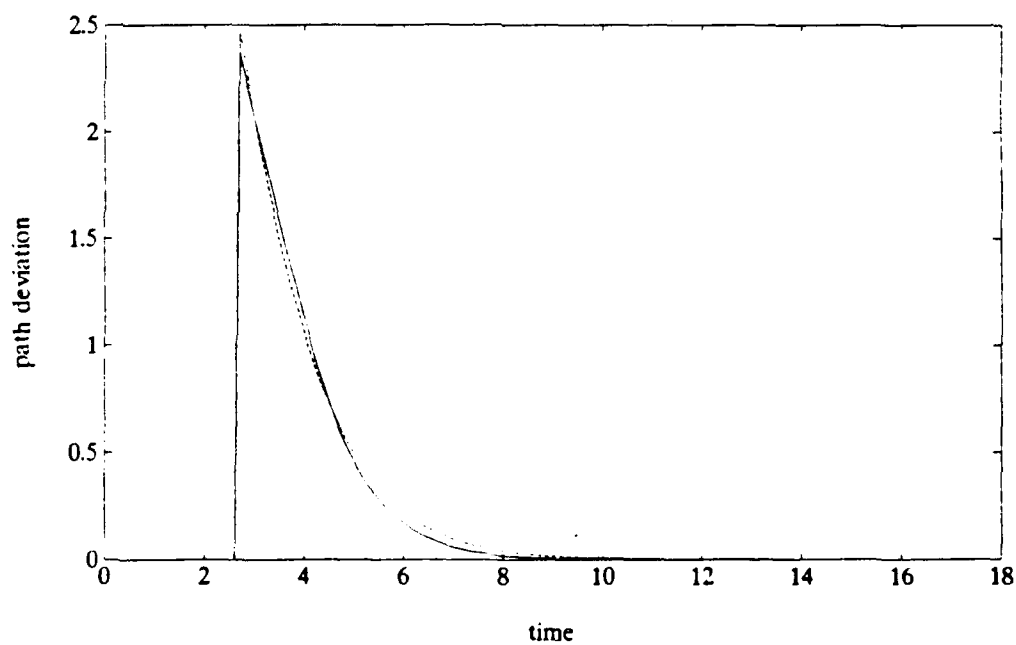
Figure 4.41 Local Path for $\alpha = 80°$
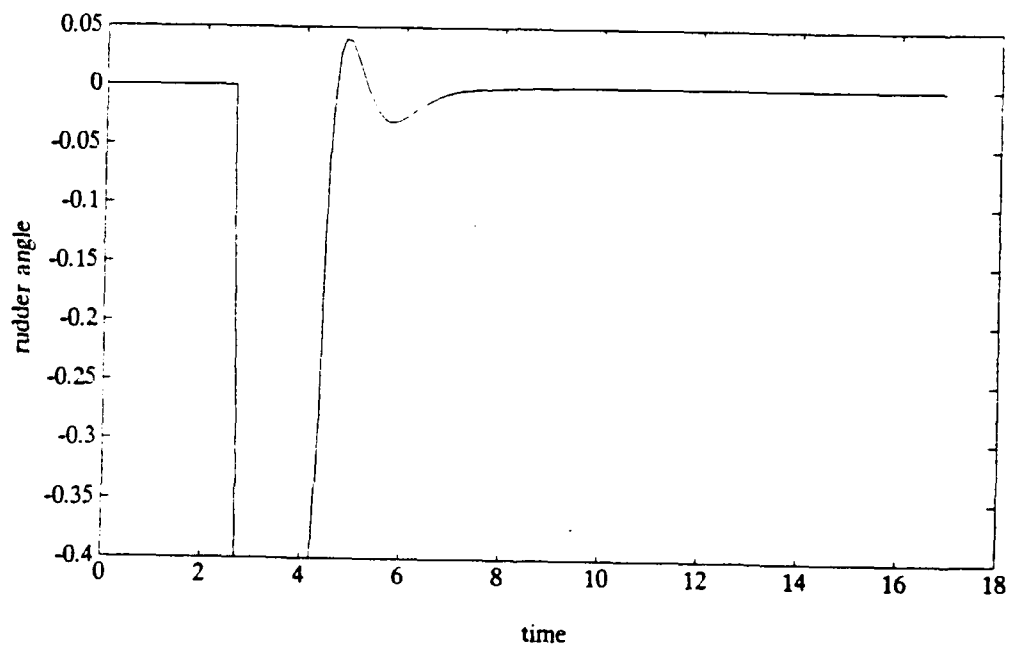
Figure 4.42 Rudder Angle for $\alpha = 80°$

CONCLUSIONS AND RECOMMENDATIONS

A. CONCLUSIONS

A method for developing a smooth reference path has been developed and presented. This technique is suitable to any type of marine vehicle and not limited to the test subject in this thesis. It has been shown that second order models are very effective in providing a smooth path between two arbitrary straight line segments. The LQR technique used is very effective in designing a control law to drive the vehicle to the reference path. Finally the turn initiation and reference path generation must conform to vehicle advance and transfer characteristics.

B. RECOMMENDATIONS

Some recommendations for further research are as follows:
- Study of the effects of sensor noise and imperfection.
- The comparison with other control/guidance schemes.

51

```
%
% ship path keeping control problem (waypoint)
%
% vehicle coefficients
%
  a11 =-1.526394;
  a12 =-0.5096502;
  a21 = 2.8750753E-02;
  a22 =-1.449505;
  b1  = 2.0674169E-03;
  b2  =-2.841506;
%
% simulation time and time step
%
  stime=500;
  deltat=0.1;
  itime=stime/deltat;
%
% damping ratio and natural frequency for the reference
path        %
  zeta=1;
  wn=1;
%
% matrices for state space control design
%
  a=[0     0      1     0    0       0;...
     0     a11    a12   0    0       0;...
     0     a21    a22   0    0       0;...
     1     1      0     0    0       0;...
     0     0      0     0    0       1;...
     0     0      0     0    -wn^2   -2*zeta*wn];
  b=[0;b1;b2;0;0;0];
%
% weighing matrices for LQR minimization
%
  q=[1     0     0     0     0    -1;...
     0     0     0     0     0     0;...
     0     0     0     0     0     0;...
     0     0     0     1    -1     0;...
     0     0     0    -1     1     0;...
    -1     0     0     0     0     1];
  r=0.1;
%
% solve riccatti equation; compute gains
%
  [k,s]=lqr(a,b,q,r);
```

```
      k1=k(1);
      k2=k(2);
      k3=k(3);
      k4=k(4);
      k5=k(5);
      k6=k(6);
%
% define waypoints and target distance
%
      ipts=3;
      target=input('target= ');
      ta=input('angle=   ');
      xdes=[0 5 5+15*cos(ta*pi/180)];
      ydes=[0 0 15*sin(ta*pi/180)];
      x1=xdes(1);
      y1=ydes(1);
      x2=xdes(2);
      y2=ydes(2);
      alpha=atan((y2-y1)/(x2-x1));
      xtotal=sqrt((x1-x2)^2+(y1-y2)^2);
%
% initial conditions
%
      psi(1)=0;
      v(1)=0;
      r(1)=0;
      y(1)=0;
      x(1)=0;
      dr(1)=0;
      yp(1)=(y(1)-y1)*cos(alpha)-(x(1)-x1)*sin(alpha);
      yr1(1)=y(1)*cos(alpha);
      yr2(1)=-tan(alpha);
      xr(1)=x(1);
      yr(1)=y(1);
      xawayf=0;
      timef=0;
      xinit=x(1);
      yinit=y(1);
      time(1)=0;
      j=1;
      istart=2;
%
% start simulation
% loop over waypoints
%
      for ipt=1:ipts-1
        x1=xdes(ipt);
        y1=ydes(ipt);
        x2=xdes(ipt+1);
        y2=ydes(ipt+1);
        x12=x2-x1;
```

```
        y12=y2-y1;
        alpha=atan((y12)/(x12));
        beta=alpha;
        alpha=abs(alpha);
        if x12 >= 0
           if y12 >=0
             alpha = alpha;
           end
           if y12 < 0
             alpha = -alpha;
           end
        end
        if x12 < 0
           if y12 >= 0
              alpha = pi-alpha;
           end
            if y12 < 0
               alpha = pi+alpha;
           end
        end
        a=(yinit-y1)*cos(alpha)-(xinit-x1)*sin(alpha);
        if a == 0;
          capt=0;
        else
           capt = +beta/(a-beta);
        end;
        yo = a/(exp(-capt)*(1+capt));
        xtotal=sqrt((x1-x2)^2+(y1-y2)^2);
  %
  %loop for each waypoint
  %
        for i=istart:itime
           time(i)=i*deltat;
           t=(i-istart)*deltat;
           j=j+1;
           if j == 10
             sim_time = time(i)
             alpha
             j=0;
           end
  %
  % equations of motion
  %
        psidot(i-1) = r(i-1);
        vdot(i-1)   = a11*v(i-1)+a12*r(i-1)+b1*dr(i-1);
        rdot(i-1)   = a21*v(i-1)+a22*r(i-1)+b2*dr(i-1);
        ydot(i-1)   = sin(psi(i-1))+v(i-1)*cos(psi(i-1));
        xdot(i-1)   = cos(psi(i-1))-v(i-1)*sin(psi(i-1));
  %
  % Euler integration
  %
```

```
        psi(i) = psi(i-1) + deltat * psidot(i-1);
        v(i)   = v(i-1)   + deltat * vdot(i-1);
        r(i)   = r(i-1)   + deltat * rdot(i-1);
        y(i)   = y(i-1)   + deltat * ydot(i-1);
        x(i)   = x(i-1)   + deltat * xdot(i-1);
        yr1(i) = yo*exp(-(t+capt))*(1+t+capt);
        yr2(i) = -(t+capt)*yo*exp(-(t+capt));
%
% coordinate changes
%
        yp(i)=(y(i)-y1)*cos(alpha)-(x(i)-x1)*sin(alpha);
        xprime=(x(i)-x1)*cos(alpha)+(y(i)-y1)*sin(alpha);
        xaway=xtotal-xprime;
        ypr=yr1(i);
        xpr=xprime;
        yr(i)=y1+xpr*sin(alpha)+ypr*cos(alpha);
        xr(i)=x1+xpr*cos(alpha)-ypr*sin(alpha);
%
% control law
%
        dr(i) = -( k1*(psi(i)-alpha)+...
                   k2*v(i)+...
                   k3*r(i)+...
                   k4*yp(i)+...
                   k5*yr1(i)+...
                   k6*yr2(i));
        if dr(i) > 0.4
            dr(i)=0.4;
        end
        if dr(i) < -0.4
            dr(i)=-0.4;
        end
%
% hit test; turn indication point
%
        xaway=xtotal-xprime;
          if xaway <= target
            istart=i+1; xinit=x(i); yinit=y(i);
            xawayf=xaway;timef=time(i);
          break, end
%
    end
    end
      dr(1)=dr(2);
%
% plot results
%

plot(x,y,xr,yr,':',xdes,ydes,'o'),xlabel('x'),ylabel('y'),..

        title('global path')
```

55

```
print
plot(time,yp,time,yr1),ylabel('path deviation'),...
    xlabel('time'),title('local path')
print
plot(time,dr),xlabel('time'),ylabel('rudder angle')

% clear
  end
```

LIST OF REFERENCES

1. Healey, A.J., et al, "Research on Autonomous Underwater Vehicles at the Naval Postgraduate School", <u>Naval Research Reviews</u>, Vol. XLIV, No. 1, 1992.

2. Papasotiriou, A., "Three Dimensional Pursuit Guidance and Control of Submersible Vehicles", <u>M.S. Thesis, Naval Postgraduate School</u>, Monterey, CA, September, 1991.

3. Chism, S., "Robust Path Tracking of Autonomous Underwater Vehicles Using Sliding Mode Control", <u>Engineers Thesis, Naval Postgraduate School</u>, Monterey, CA, December 1990.

4. Crane, C.L., Eda, H., and Landsburg, A., "Controllability", in <u>Principles of Naval Architecture</u>, SNAME, 1989.

5. Freidland, B., <u>Control System Design</u>, McGraw-Hill, Inc., 1986.

INITIAL DISTRIBUTION LIST

1. Defense Technical Information Center   2
   Cameron Station
   Alexandria, VA 22304-6145

2. Library, Code 52   2
   Naval Postgraduate School
   Monterey, CA 93940-5000

3. Chairman, Code ME   1
   Department of Mechanical Engineering
   Naval Postgraduate School
   Monterey, CA 93940-5000

4. Naval Engineering Curricular Office, Code 34 1
   Naval Postgraduate School
   Monterey, CA 93940-5000

5. LT Timothy J. Panoff   5
   Department Head Class 126
   Surface Warfare Officers School Command
   Newport, RI 02841-5012

6. Professor F. A. Papoulias, Code MEPa   4
   Department of Mechanical Engineering
   Naval Postgraduate School
   Monterey, CA 93940-5000